

# NAVAL POSTGRADUATE SCHOOL MONTEREY, CALIFORNIA



## THESIS

**COASTALLY TRAPPED DISTURBANCES  
ALONG THE U. S. WEST COAST: SYNOPTIC AND  
MESOSCALE ANALYSIS OF 9 - 12 JUNE 1994**

by

Paul S. Oosterling

September, 1995

Thesis Advisor:

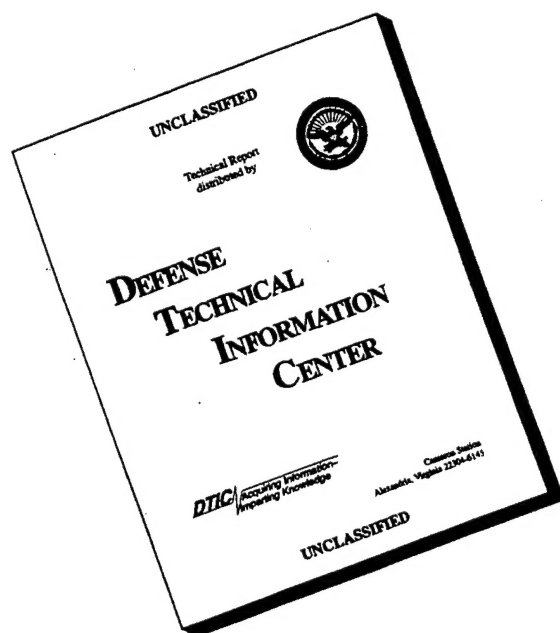
Wendell A. Nuss

Approved for public release; distribution is unlimited.

19960327 075

DTIC QUALITY INSPECTED 1

# DISCLAIMER NOTICE



**THIS DOCUMENT IS BEST QUALITY AVAILABLE. THE COPY FURNISHED TO DTIC CONTAINED A SIGNIFICANT NUMBER OF PAGES WHICH DO NOT REPRODUCE LEGIBLY.**

| REPORT DOCUMENTATION PAGE  |   |  | Form Approved OMB No. 0704-0188                   |   |
|--|---|--|---|---|
| Public reporting burden for this collection of information is estimated to average 1 hour per response, including the time for reviewing instruction, searching existing data sources, gathering and maintaining the data needed, and completing and reviewing the collection of information. Send comments regarding this burden estimate or any other aspect of this collection of information, including suggestions for reducing this burden, to Washington Headquarters Services, Directorate for Information Operations and Reports, 1215 Jefferson Davis Highway, Suite 1204, Arlington, VA 22202-4302, and to the Office of Management and Budget, Paperwork Reduction Project (0704-0188) Washington DC 20503.  |   |  |   |   |
| 1. AGENCY USE ONLY (Leave blank)   |   | 2. REPORT DATE<br>September 1995                             |   | 3. REPORT TYPE AND DATES COVERED<br>Master's Thesis |
| 4. TITLE AND SUBTITLE<br>COASTALLY TRAPPED DISTURBANCES<br>ALONG THE U. S. WEST COAST: SYNOPTIC AND MESOSCALE<br>ANALYSIS OF 9 - 12 JUNE 1994.   |   |  | 5. FUNDING NUMBERS                                |   |
| 6. AUTHOR(S)<br>Oosterling, Paul S.  |   |  |   |   |
| 7. PERFORMING ORGANIZATION NAME(S) AND ADDRESS(ES)<br>Naval Postgraduate School<br>Monterey CA 93943-5000  |   |  | 8. PERFORMING<br>ORGANIZATION<br>REPORT NUMBER    |   |
| 9. SPONSORING/MONITORING AGENCY NAME(S) AND ADDRESS(ES)  |   |  | 10. SPONSORING/MONITORING<br>AGENCY REPORT NUMBER |   |
| 11. SUPPLEMENTARY NOTES The views expressed in this thesis are those of the author and do not reflect the official policy or position of the Department of Defense or the U.S. Government.   |   |  |   |   |
| 12a. DISTRIBUTION/AVAILABILITY STATEMENT<br>Approved for public release; distribution is unlimited.  |   |  | 12b. DISTRIBUTION CODE                            |   |
| 13. ABSTRACT (maximum 200 words)<br>Synoptic and mesoscale analyses were made for a coastally trapped disturbance along the central California coast that occurred on 9 - 12 June 1994. Hourly sea-level pressure analyses were constructed using a Multi-Quadric interpolation technique to blend observations with synthetic observations from the National Meteorological Center mesoscale model in data-void regions over the ocean. In addition to describing the disturbance's evolution in terms of sea-level pressure changes, the 850 mb temperature change and thermal advection were analyzed to determine their influence on the initiation and propagation of the coastally trapped disturbance. Low-level thermal advection was shown to be a key mechanism in initiating the event, in the development of an off-shore low pressure center, and subsequently in changing the nature of the forcing of the disturbance from ageostrophic down-gradient flow to more nearly a response to the existing geostrophic pressure gradient. |   |  |   |   |
| 14. SUBJECT TERMS<br>Coastally Trapped Disturbance, Synoptic and Mesoscale Analysis, Low-Level Thermal Advection, Ageostrophic Down-Gradient Flow, Geostrophic Response.   |   |  | 15. NUMBER OF<br>PAGES<br>85                      |   |
|  |   |  | 16. PRICE CODE                                    |   |
| 17. SECURITY CLASSIFI-<br>CATION OF REPORT<br>Unclassified   | 18. SECURITY CLASSIFI-<br>CATION OF THIS PAGE<br>Unclassified | 19. SECURITY CLASSIFI-<br>CATION OF ABSTRACT<br>Unclassified | 20. LIMITATION OF<br>ABSTRACT<br>UL               |   |



Approved for public release; distribution is unlimited.

**COASTALLY TRAPPED DISTURBANCES ALONG THE U. S. WEST  
COAST: SYNOPTIC AND MESOSCALE ANALYSIS OF 9 - 12 JUNE 1994**

Paul S. Oosterling  
Lieutenant, United States Navy  
B.S., Florida Institute of Technology, 1986

Submitted in partial fulfillment  
of the requirements for the degree of

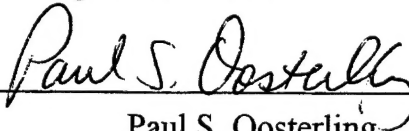
**MASTER OF SCIENCE IN METEOROLOGY AND PHYSICAL  
OCEANOGRAPHY**

from the


**NAVAL POSTGRADUATE SCHOOL**

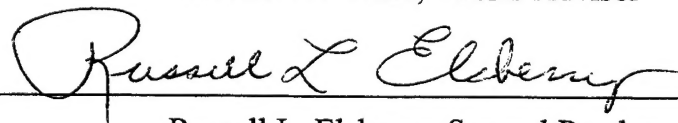
**September 1995**

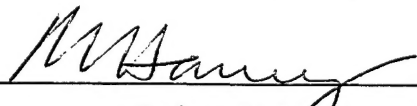
Author:

  
Paul S. Oosterling

Approved by:

  
Wendell A. Nuss, Thesis Advisor

  
Russell L. Elsberry, Second Reader

  
Robert L. Haney, Chairman  
Department of Meteorology



## ABSTRACT

Synoptic and mesoscale analyses were made for a coastally trapped disturbance along the central California coast that occurred on 9 - 12 June 1994. Hourly sea-level pressure analyses were constructed using a Multi-Quadric interpolation technique to blend observations with synthetic observations from the National Meteorological Center mesoscale model in data-void regions over the ocean. In addition to describing the disturbance's evolution in terms of sea-level pressure changes, the 850 mb temperature change and thermal advection were analyzed to determine their influence on the initiation and propagation of the coastally trapped disturbance. Low-level thermal advection was shown to be a key mechanism in initiating the event, in the development of an off-shore low pressure center, and subsequently in changing the nature of the forcing of the disturbance from ageostrophic down-gradient flow to more nearly a response to the existing geostrophic pressure gradient.





## TABLE OF CONTENTS

|  |    |
|--|----|
| I. INTRODUCTION .....  | 1  |
| II. DATA/OBSERVATIONS .....                                  | 5  |
| A. COASTAL METEOROLOGY ACCELERATED RESEARCH INITIATIVE ..... | 5  |
| 1. Surface Observations .....                                | 6  |
| 2. Upper Air .....   | 6  |
| B. MONTEREY AREA SHIP TRACK (MAST) EXPERIMENT .....          | 7  |
| III. ANALYSIS METHODS AND PROCEDURES .....                   | 9  |
| A. OBJECTIVE ANALYSIS METHOD .....                           | 9  |
| 1. Multiquadric Technique .....                              | 9  |
| 2. Sea-Level Pressure Analysis Method: Blending .....        | 11 |
| 3. Upper-Air Analysis .....                                  | 13 |
| B. DISPLAY - DIAGNOSTIC PROGRAM .....                        | 14 |
| VI. SYNOPTIC/MESOSCALE ANALYSIS .....                        | 17 |
| A. SYNOPTIC EVOLUTION .....                                  | 17 |
| 1. Pre-Initiation Phase .....                                | 18 |
| 2. Initiation Phase .....                                    | 24 |

|     |  |    |
|-----|--|----|
| 3.  | Propagation Phase .....  | 33 |
| 4.  | Decay Phase .....  | 39 |
| 5.  | Evolution of the Coastally Trapped Disturbance and Wind Pattern<br>Summary ..... | 45 |
| B.  | SYNOPTIC-SCALE INFLUENCES ON SEA-LEVEL PRESSURE ..                               | 47 |
| 1.  | 850 MB Temperature Changes and Sea-Level Pressure Evolution<br>.....             | 47 |
| 2.  | Thermal Advection and 850 MB Temperatures .....                                  | 55 |
| V.  | DISCUSSION .....   | 65 |
| A.  | INITIATION MECHANISM .....   | 65 |
| B.  | MARINE BOUNDARY LAYER INFLUENCE .....  | 67 |
| VI. | CONCLUSION AND REMARKS .....   | 71 |
|     | LIST OF REFERENCES .....   | 73 |
|     | INITIAL DISTRIBUTION LIST .....  | 75 |

## I. INTRODUCTION

With the United States Navy's focus shifted from a global threat or a "Blue Water" force to regional challenges in the coastal or littoral zone, the job of predicting accurately the environmental conditions affecting operations has become much more difficult. Attaining a better understanding of the atmospheric dynamics and complex interactions taking place in such a diverse environment is paramount to conducting operations in a safe and successful manner. The coastal region is an area that poses varying technical and tactical challenges to Naval Forces conducting such actions as amphibious landings, missile launches, and flight operations. An enhanced understanding of the factors affecting visibility, temperature, and winds in the coastal region will enable the United States Navy to better meet their goals. This research examines a coastal regional phenomena on the west coast of the United States as a prototype for the types of meteorological conditions that need to be forecast.

One of the most dramatic changes in the persistent warm season environmental conditions on the west coast of the United States has been termed a "southerly surge" or a coastally trapped disturbance (CTD). Several times a year, the predominantly northwesterly winds along the U.S. west coast are abruptly interrupted by a transition to southerly winds. The transition takes place within a few hundred kilometers of the coast and may persist for several days. Preceding the event, a period of off-shore flow clears the coastal stratus and fog that dominates in the northwest wind regime, and additionally reduces the marine

boundary layer to a minimum. This CTD event is very often accompanied by a rapid increase in the depth of the marine boundary layer, formation of fog and low stratus, decreasing temperatures and visibilities, and rising pressures (Bond et al. 1995). These rapidly changing conditions have an obvious and significant effect on normal shipboard operations. On most occasions, the advance of the southerly surge can be tracked by satellite pictures. The characteristic CTD signature is a narrow tongue of fog and stratus progressing from south to north along the coast. It has been shown that the surge and stratus signature are restricted to approximately one Rossby radius of deformation ( $\sim 100\text{-}200$  km) from the coast (Bond et al. 1995), which suggests that it is coastally trapped.

The progression of the southerly transition has been ascribed to a variety of mechanisms: rotationally trapped Kelvin waves (Dorman 1985; Reason and Steyn 1992), trapped gravity currents (Dorman 1987; Mass and Albright 1987), and ageostrophic down-gradient flow forced by the along-barrier synoptic-scale pressure gradient (Mass and Albright 1987, 1988). In each case, the orographic boundaries of the coastal mountain range play an extremely important role. If the marine layer, in which the stratus transition takes place, is at a height lower than the coastal mountain crests, then the transition is confined vertically by the inversion and laterally by the Coriolis force trapping the flow against the mountains (Reason and Steyn 1992). The Kelvin wave and trapped gravity current theories are remarkably similar in their dynamic mechanism. Both theories indicate the CTD develops as a manifestation of coastal marine boundary layer (MBL) height changes. If the synoptic gradient is weak enough, the Kelvin wave and trapped gravity

current interpretations state that height changes in the MBL are responsible for the reversal in the along-shore pressure gradient, which allows the surge to progress northward along the coast. By contrast, the synoptically forced interpretation is that atmospheric characteristics above the MBL dominate the along-shore pressure gradient reversal, and thus force the surge from the south.

Irrespective of the dynamic mechanism for the northward progression of the stratus in the marine layer, all agree that in order for the transition to occur, certain synoptic conditions must precede the event: high pressure over the eastern Pacific Ocean must slowly build and ridge across the northwestern United States (Oregon and Washington), and a persistent heat low or trough deepens over the valleys in central California. The resulting synoptic situation results in a period of offshore flow across the dominant coastal topography along central and northern California, which causes adiabatic down-slope warming and the formation of a lee trough on the seaward side of the mountains. The continued down-gradient warming, or lee troughing, draws the central valley heat low offshore, which adds to pressure falls in this region and generates a small but distinct along-shore pressure gradient reversal.

Each of the three explanations for the CTD dynamics suffer from several deficiencies. The Kelvin wave and gravity current explanations do not adequately address the initiation mechanisms, while the synoptic-scale explanation does not address propagation. These deficiencies are due in part to a lack of a complete observation set over the life cycle of a CTD. A central issue to understanding these events is gaining a detailed

synoptic-scale evolution and then understanding how it affects the MBL. Specific questions are:

- i) Can synoptic-scale evolution explain the northward propagation of the southerly surge?
- ii) What are the synoptic-scale processes that cause the along-shore pressure changes over a complete life cycle?
- iii) How large are the pressure changes caused by the marine boundary layer depth changes (key to the Kelvin wave and gravity current hypotheses) and are they required to force southerly winds?
- iv) What are the relative roles of the marine boundary layer processes and the synoptic-scale in the along-shore pressure gradient changes?

The aim of this study is to examine the relationships among the synoptic-scale flow, the coastal topography, and sea-level pressure changes associated with the initiation and evolution of a CTD. The relative roles of lee troughing and thermal advection in changing the synoptic-scale pressure pattern will also be examined. Our approach is to utilize various analysis schemes and diagnostic tools on an available data set that was collected during the summer of 1994 as part of a coastal meteorology study along the central California coast.

## **II. DATA/OBSERVATIONS**

The coastal mountains that extend along virtually the entire length of the U.S. west coast represent a barrier to the lower-tropospheric flow. Their interaction with the synoptic-scale flow gives rise to a variety of mesoscale, trapped, atmospheric phenomena within approximately 100 km of the coastline. These features greatly influence the weather of the coastal zone. Unfortunately, they are not resolved adequately by the present observational network, and current operational numerical weather prediction (NWP) models are unable to realistically simulate their evolution. A number of theoretical ideas have been proposed to explain the mesoscale features of the coastal zone, but few have been tested with data sets of sufficient completeness or resolution.

### **A. COASTAL METEOROLOGY ACCELERATED RESEARCH INITIATIVE**

In the summer of 1994, the Office of Naval Research Coastal Meteorology Accelerated Research Initiative (ARI) sponsored a field program that involved the Naval Postgraduate School, the National Oceanographic and Atmospheric Administration (NOAA), Scripps Institute of Oceanography, and San Diego State University. The program entailed three months of dedicated studies in the central California coastal region. Although the program studied an area north of Point Conception and south of the Oregon border, the primary focus was on the central California (CA) coast near Monterey Bay. A complex network of observing stations was set up to augment the existing routine observational network. The additional stations were placed in various regions for specific intervals to

observe any trapped disturbances with adequate time and spatial resolutions. During the three-month period, a single coastally trapped disturbance (CTD) occurred between 9 June and 12 June 1994. Surface and upper-air observations from these three days were used in this study to characterize the synoptic and mesoscale evolution of the CTD.

### **1. Surface Observations**

Surface observations included the routine hourly surface airways reports, routine ship reports, moored buoy and Coastal Marine Automated Network (C-MAN) station reports, and California Department of Forestry (CDF) station reports. Surface observations were used to characterize the sea-level pressure evolution preceding and during the event to understand the synoptic and mesoscale evolutions and interactions throughout the CTD. The spacing of these sites is sufficient to define the synoptic and mesoscale pressure change on an hourly basis. This time and space resolution is essential for testing the hypothesis that the initiation of the CTD is due to the resonant synoptic-scale forcing, relaxation of the along-coast pressure gradient, and the development of a lee trough.

### **2. Upper Air**

Upper-air observations consisted of radar wind profilers along the coast, operational and special rawinsonde launches, and aircraft measurements. Special daily soundings were taken at Monterey and Fort Hunter Liggett at 12UTC and 15UTC respectively. These soundings supplemented the routine soundings taken at Vandenberg AFB, Oakland, and elsewhere. The 915Mhz profilers were located near the coast at Monterey, Santa Cruz, Hollister, Ft. Bragg, Crescent City, and Medford. These profilers provided hourly winds to



nearly 3 km and most sites provided virtual temperature profiles to near 1.5 km.

## **B. MONTEREY AREA SHIP TRACK (MAST) EXPERIMENT**

In addition to the observations noted above, supplementary measurements were taken during the month of June 1994 as part of the Monterey Area Ship Tracks (MAST) Experiment (Durkee 1994). Shipboard soundings, surface observations, and multiple aircraft flights were undertaken as part of that experiment. Some of the ship surface observations and soundings were also used in these analyses.



### **III. ANALYSIS METHODS AND PROCEDURES**

Using all available data from the Coastal Meteorology ARI field study for the period from 9 June through 12 June 1994, objective surface and upper-air analyses were constructed and used in several diagnostic calculations to accomplish the following:

- i) describe the synoptic and mesoscale sea-level pressure evolution during a coastally trapped disturbance;
- ii) relate the pressure tendencies to the onset of the southerly transition;
- iii) identify synoptic-scale and marine boundary layer causes of along-shore sea-level pressure changes during the event; and
- iv) determine the role of the atmospheric evolution above the marine boundary layer in the formation and evolution of a lee trough, and sea-level pressure changes due to thermal advection.

#### **A. OBJECTIVE ANALYSIS METHOD**

##### **1. Multiquadric Technique**

To generate an accurate mesoscale representation of the hourly sea-level pressure (SLP) patterns and its evolution throughout the event, objective SLP analyses were derived using the multiquadric (MQ) technique described by Nuss and Titley (1994). The foundation for multiquadric interpolation, as well as statistical interpolation and the method of Caracena (1987), lies within the general theory of interpolation using radial basis functions. The interpolation equation using radial basis functions is

$$H(X) = \sum \alpha_i Q(X - X_i), \quad (1)$$

where  $H(X)$  is a spatially varying field, such as SLP, and  $Q(X - X_i)$  is a radial basis function in which the argument represents the vector between an observation point  $X_i$  and any other point in the domain. The coefficients  $\alpha_i$  are weighting factors that must be determined from the observations or specified in some manner. The multiquadric method uses hyperboloid functions as the basis functions in the form

$$Q(X - X_i) = - \left( \frac{\|X - X_i\|^2}{c^2} + 1.0 \right)^{1/2}, \quad (2)$$

where  $c$  is an arbitrary, and typically, small constant. This form of the multiquadric basis function is a member of the general class of multiquadric functions described by Madych and Nelson (1990) and gives similar results to the original form. The constant  $c$  is termed the multiquadric parameter. To determine the coefficients  $\alpha_i$  a set of linear equations must be solved. Applying the interpolation equation to the field at every observation point  $(x_i, y_i)$  results in the following set of equations:

$$H(x_i, y_i) = \sum_{j=1}^N \alpha_j Q_j(x_i, y_i), \quad (3)$$

where

$$Q_j(x_j, y_j) = - \left( \frac{|x_j - x_i|^2 + |y_j - y_i|^2}{c^2} + 1.0 \right)^{1/2}. \quad (4)$$

Note that the observation  $H(x_i, y_i)$  may represent either the raw observation or the deviation of the observation from some background field. Deviations from the mean of the observations are analyzed and then the mean is added to the solution. Since equation (4) applies at the  $N$  observation points, this results in a set of  $N$  equations with  $N$  unknown coefficients  $\alpha_i$  that are determined using standard techniques as explained in Nuss and Titley (1994).

## **2. Sea-Level Pressure Analysis Method: Blending**

A major obstacle in generating an accurate synoptic field evolution of the SLP for the days of the CTD event was in the distribution of data in the coastal region. The data have an extremely abrupt transition from a dense field of observations over land to a very sparse data set over the ocean, which produces problems for simple analysis techniques. To overcome this problem, the MQ technique was used to blend the observational data into the gridded fields of the National Meteorological Center mesoscale ETA model. The ETA model was chosen from the available operational models because it had the highest spatial resolution (80 km) and appeared to be most accurate in daily operational performance.

This blending of the model and observation fields was utilized to obtain the best analysis by using the ETA model values in the data-sparse regions. Since the desire was to use the ETA model values only to fill in the data holes in the operational data, a sphere of influence was calculated around each grid point during the blending process. Thus, one of the variable parameters for the blending is this region of influence. For this study, the parameter was set so that an ETA model value would be inserted at the grid point if there

was no real observation within five grid points (100 km).

A goal of blending the ETA model fields with the interpolated observation field was to ensure that the shipboard observations (maximum numbers on the synoptic hours - 00UTC, 06UTC, 12UTC, 18UTC) would have the greatest influence on the final analyses. The ETA model analyses were only available at 12-h intervals (00UTC and 12UTC). Blended SLP analyses were first completed at the 06UTC and 18UTC synoptic hours using a linear interpolation of the ETA model between the 00UTC and 12UTC analysis times for the first-guess fields. Hourly blended first-guess SLP fields were then created by linearly interpolating the 6-h blended analyses.

The MQ technique described in Nuss and Titley (1994) applies specifically to observations without error. Obviously, the observational data set used in this study contained errors. Each routine hourly airways reporting station was assigned a site-specific error while the shipboard observations and the inserted ETA model points were assigned a general error value. Observational error characteristics were estimated by calculating the root mean square (RMS) deviation of each of the observations compared to the first-guess field over a 3-month period. A data smoothing parameter was specified from this observational error estimate. A data threshold was set at 6.0, which results in all observations with a difference of greater than 6 mb from the first-guess field in a particular analysis being excluded from that analysis. Observational deviations of less than 6 mb were retained and their site-specific error was used to set the smoothing parameter for each observation. The calculation of the RMS error was completed for each observing station

over the three month experiment period to determine any bias in the data and to ensure an accurate and current representative RMS error was utilized. The error terms were added to the matrix diagonal terms (Eq. 4) to produce the required smoothing.

For model grid points used as observations to fill data holes, a model error was calculated using the smoothing parameter (set at 0.01) and the RMS error of the first-guess field. The error for these model observations was calculated with the simple formula

$$(1.0 - 0.01) * RMS, \quad (5)$$

where RMS stands for the root mean square deviation of the model first-guess from the real observations calculated over the entire domain for a specific analysis time. These error values were then added into the matrix diagonal terms as previously described.

Numerous trial analyses were completed to determine the best combination of parameter values to produce the most accurate series of SLP analyses. The accuracy was determined subjectively by finding the SLP analysis series that best captured the influence of the observations and maintained features in sufficient detail on the 20 km grid.

### **3. Upper-Air Analysis**

The same technique for generating the SLP analyses was employed for generation of wind and temperature analyses at the standard levels of 850 mb, 700 mb, and 500 mb. Due to the limited upper-air observations in space and time, these analyses fields were only generated for the synoptic times of 00UTC and 12UTC.

The free variables of model and data smoothing, and grid point radius of influence were altered to maintain the upper-air observation characteristics. The model smoothing value was set at 0.001, based on equation (5), where the same observational error is used for each observation and is set at 1.0. The data threshold was set at 7.0 ( $^{\circ}\text{K}$ ,  $\text{ms}^{-1}$ ) for both temperature and winds. The radius of influence for the grid points was set at 30. That is, an ETA model value was inserted only if there was no real observations within 30 grid points (600 km).

## **B. DISPLAY - DIAGNOSTIC PROGRAM**

All MQ analyses were displayed by a program called VISUAL, which is a diagnostic and display program that uses Graphic Kernel System (GKS) primitives and National Center for Atmospheric Research (NCAR) graphics utility routines to examine meteorological grids and observations. The program extensively uses the GKS plot segmentation and graphical input capabilities and is primarily intended to be used interactively to explore data sets.

Gridded data sets on either Lambert Conformal, Polar Stereographic, or Mercator grids are acceptable for input and satellite images may be overlaid on the plots. Gridded analysis or forecast fields and satellite image fields use a standard developed for VISUAL and observation files use the GEMPAK format.

The program was initially developed by W. Nuss while at NCAR. The program can accept data of many types: sea-level pressure, temperatures in vertical levels, sea-surface temperature, geopotential height, moisture, wind components, terrain elevation, surface pressure, and vertical motion. Satellite image data files must be GOES imagery and be in



the PC-McIdas format.

In this study, VISUAL was used to display the SLP analyses and to perform SLP field subtractions to generate pressure tendency plots. In addition, upper-level temperature and wind analyses were used to generate thermal advection charts. Finally, along-shore soundings were plotted to gain a representation of the changes in the marine boundary layer during the CTD event.



## **VI. SYNOPTIC/MESOSCALE ANALYSIS**

### **A. SYNOPTIC EVOLUTION**

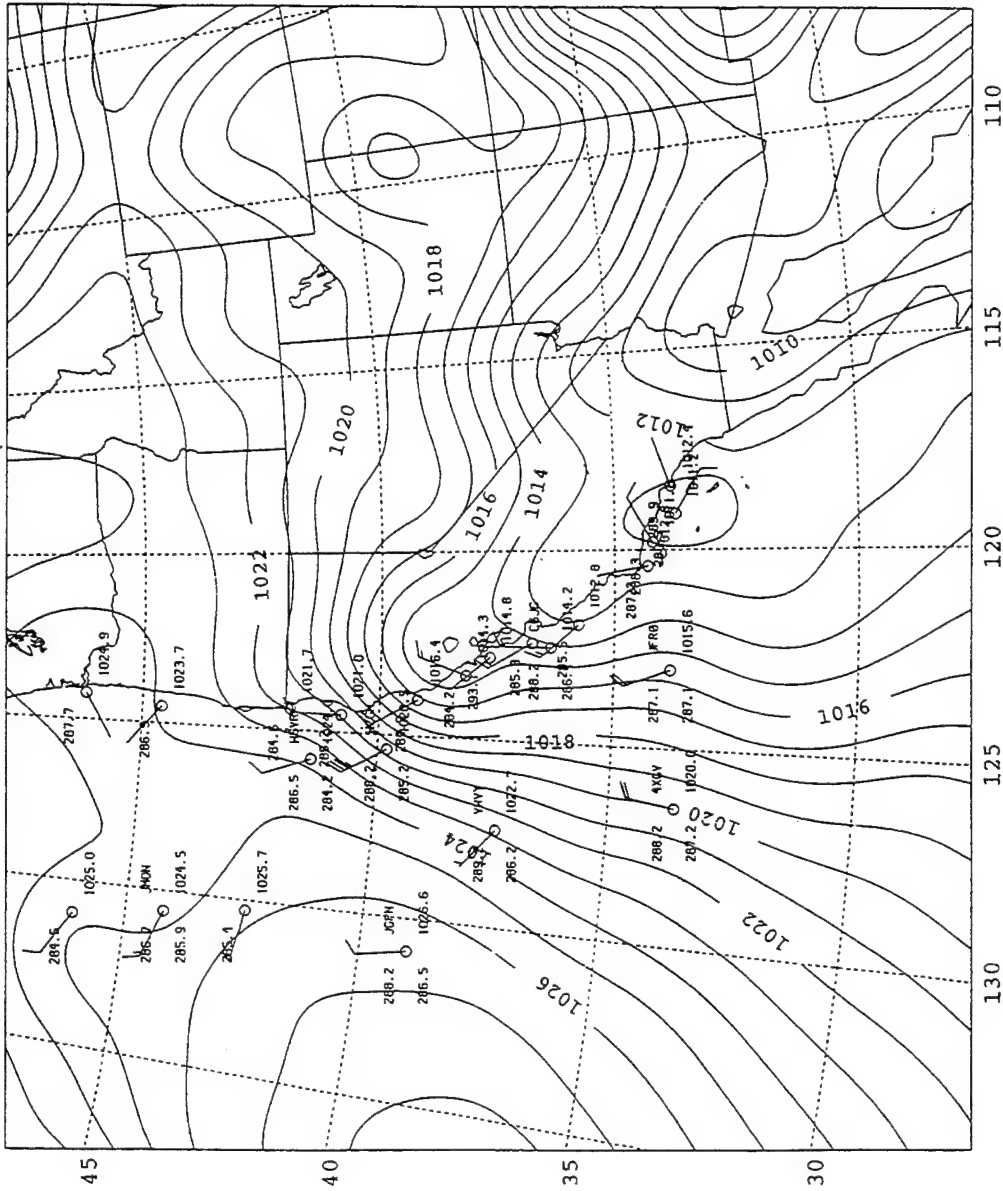
The CTD of 9-12 June 1994 has been divided into four distinct phases to best illustrate its evolution. The pre-initiation phase (00UTC 9 June through 00UTC 10 June) is associated with changes in the state of the atmosphere that permitted the formation and progression of a CTD. During the pre-initiation phase, a thermal trough over California moved westward to the California coast and higher pressures began to ridge across southern California as stratus developed in the region. The initiation phase (06UTC-12UTC 10 June) describes the atmospheric evolution during the start and initial progression of the CTD. During the initiation phase the thermal trough moved off-shore around 06UTC 10 June, and higher pressures and stratus continued to develop to the south. These two features acted in concert to produce an along-shore SLP gradient reversal from south to north that then initiated the surge. The propagation phase (15UTC 10 June - 12UTC 11 June) details the period when the CTD freely propagated to the north along the central California (CA) coast. During this phase the along-shore SLP gradient remained south to north, and an area of low pressure developed off the central coast, which favored continued progression of the surge. The decay phase (15UTC 11 June - 00UTC 12 June) describes the decay of the favorable CTD conditions, which included a weakening of the along-shore SLP and the thermal trough, and the shifting of the coastal surface winds back to the climatological northerly flow.

## **1. Pre-Initiation Phase**

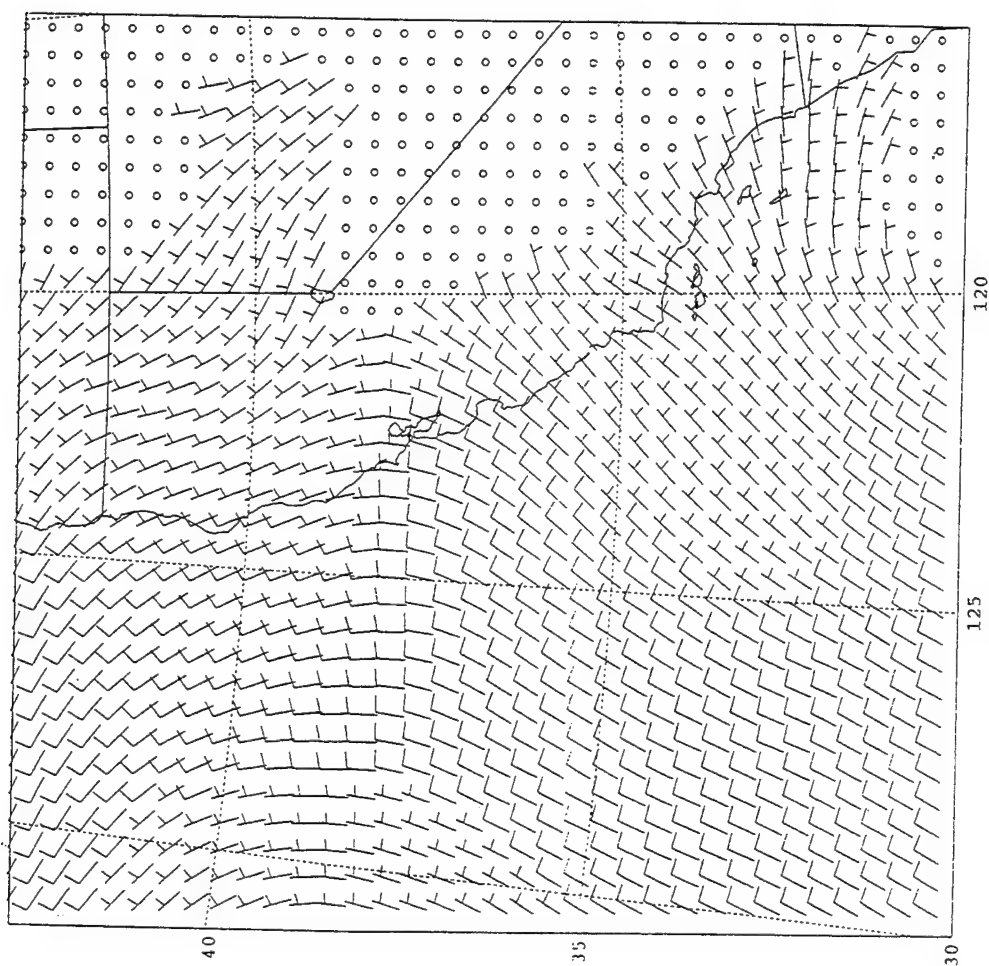
Between 00UTC and 12UTC 9 June, high pressure over the eastern Pacific ridged across the northwestern U. S. and the thermal trough over the central valley of California moved west toward the coast, with a north-to-south orientation as indicated in the SLP analysis for 12UTC 9 June (Fig. 1). The along-coast SLP gradient was significantly weakened from Pt. Arena to southern CA due to the presence of the thermal trough along the coast. Surface wind observations in Fig. 1 are northerly along most of the coast, which is consistent with the SLP gradient on the west side of the trough axis. To initiate a CTD, the southward directed along-coast SLP gradient must be reversed by the migration of the coastal thermal trough farther off-shore to the north.

The 850 mb winds at 12UTC 9 June have a strong off-shore component along the coast from San Francisco (SFO) to San Diego (Fig. 2), which is conducive to the formation of lee troughing along the coastal mountains and which may account for the trough axis shifting toward the coast during the previous 12 h. North of SFO, the winds are northwesterly with an on-shore component. The 500 mb heights (Fig. 3) at 12UTC 9 June have a broad ridge with its axis along the southern California coast and extending farther to the northwest across the eastern Pacific. This upper-level ridge is coincident with the eastern Pacific surface high pressure area (Fig. 1).

From 15UTC 9 June (Fig. 4) through 00UTC 10 June (Fig. 5), the pressure gradient along the central CA coast weakened as the thermal trough began to expand off-shore between Monterey (MRY) and Pt. Conception. This is clearly shown in the 00UTC 10 June



**Figure 1.** SLP analysis (solid lines, 1 mb interval) for 12UTC June 1994, using MQ technique to blend obs with ETA values (data voids). Selected ship and buoy observations: Temperature and dew point ( $^{\circ}\text{C}$ ) full wind barb 10 kt, half barb 5 kt.



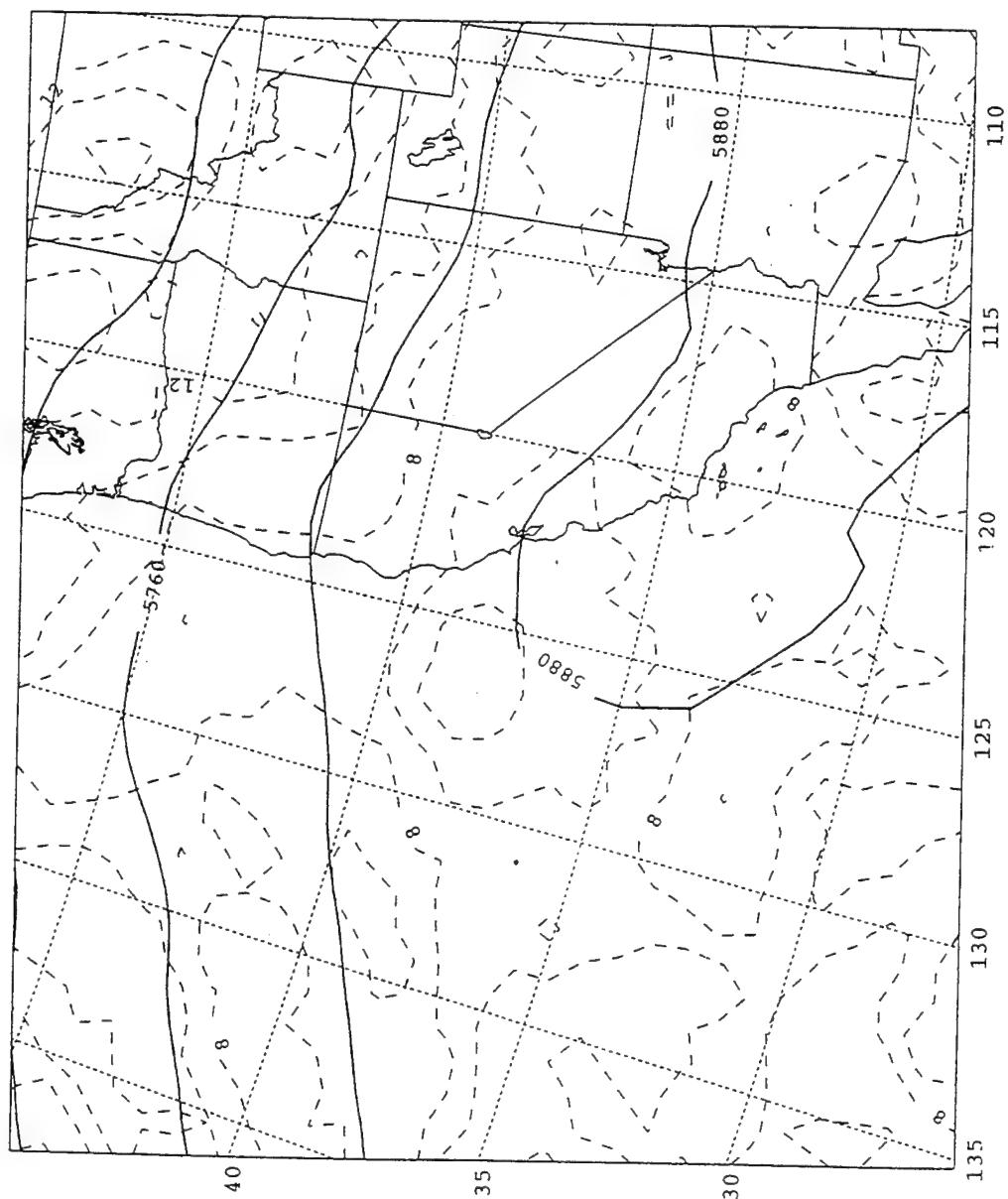


**Figure 3.** ETA model 500 mb geopotential height (solid lines, 60 m interval) and vorticity (dashed lines,  $2 \times 10^{-5} \text{ s}^{-1}$  intervals) for 12UTC 9 June.

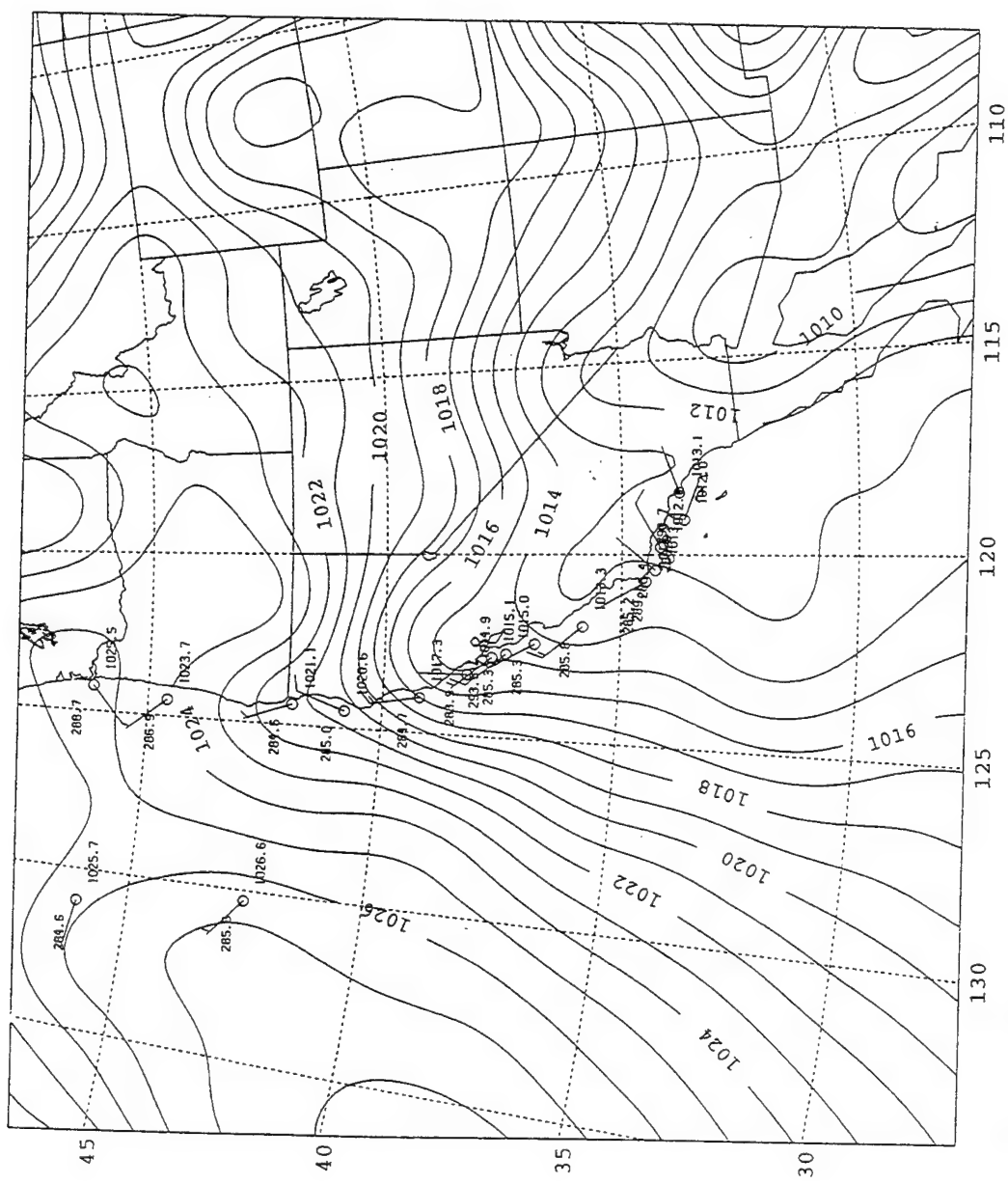
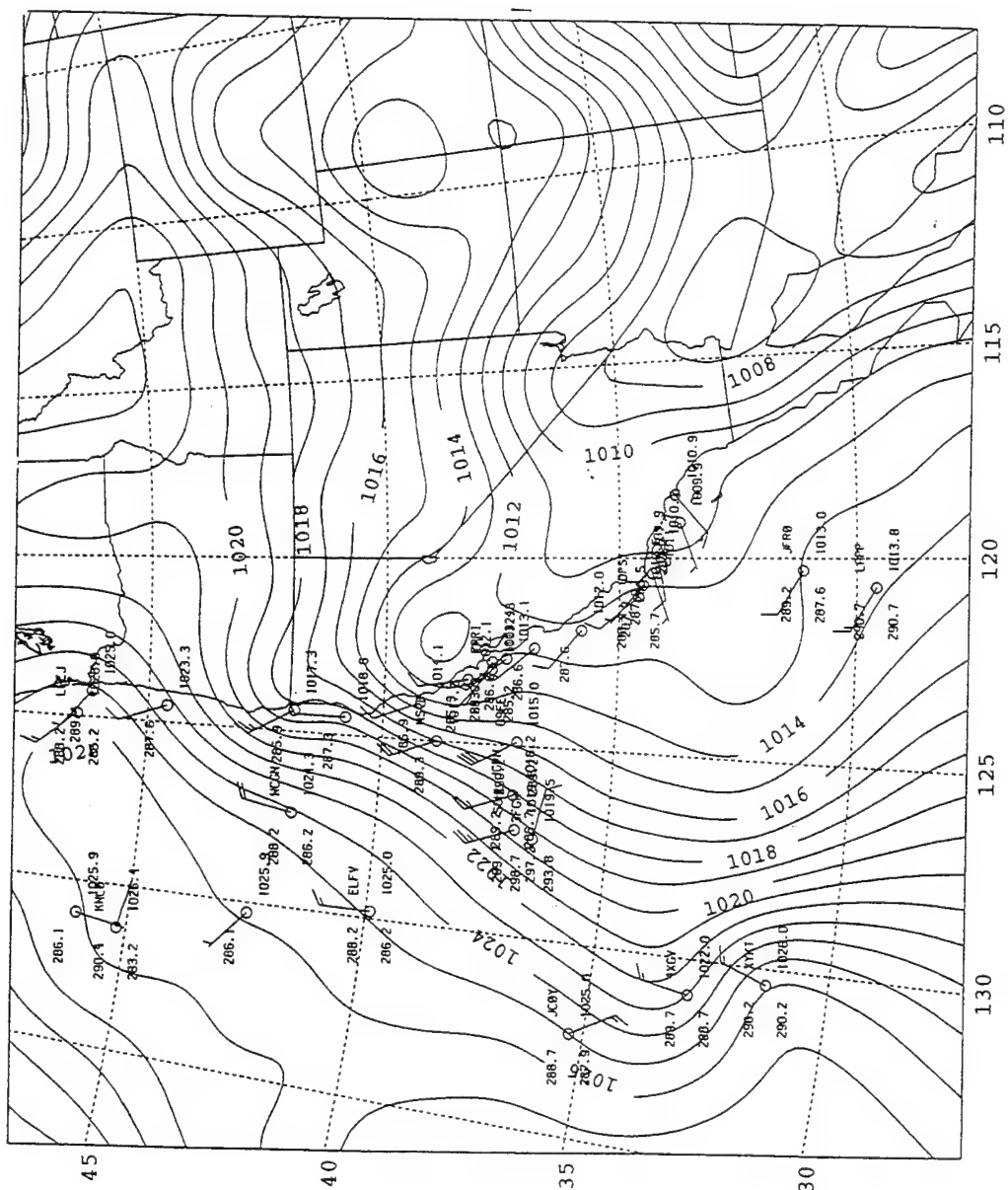


Figure 4. Blended SLP analysis as in Fig. 1, except for 18 UTC 9 June 1994.





**Figure 5.** Blended SLP analysis as in Fig. 1, except for 00UTC 10 June 1994.

SLP analysis with the trough axis still inland, but a broad area of weaker pressure gradient extending off-shore from the coast south of Monterey. At the same time, a stronger cross-coast pressure gradient developed south of the Channel Islands, and from inspection of the series of visible satellite imagery (not shown), an increase in the spatial coverage of stratus in the region was observed. An eddy feature is apparent in the surface winds as well as the visible image (Fig. 6) suggestive of the development of a Catalina Eddy.

During the previous 12 h, the 850 mb winds have shifted from northeasterly to southeasterly along the coast south of Monterey (Fig. 7). The 850 mb winds are light ( $<2$  kt) across the MRY area and remain northerly north of SFO. This 850 mb wind pattern is associated with the northward movement of a low-level cyclonic circulation off the coast (Fig. 7). Although the position of this feature is uncertain due to the lack of off-shore observations, the coastal wind shift is documented with upper-air observations along the coast. The 500 mb height analysis from the ETA model (Fig. 8) indicates that the ridge has amplified and shifted slowly east with its axis across the Pacific Northwest. To the south of the CA coast, the ridge has also broadened in extent since 12UTC 9 June.

## **2. Initiation Phase**

The CTD was initiated at 06UTC 10 June as a reversal in the along-shore SLP gradient, which is documented by the coastal observations between the buoy south of Monterey and other buoys in the California Bight (CB) region (Fig. 9). Whereas the surface pressure south of Monterey is 1010.2 mb, the pressure in the Channel Islands is  $\sim 1011.5$  mb. The thermal trough has extended far enough off-shore north of Pt. Conception

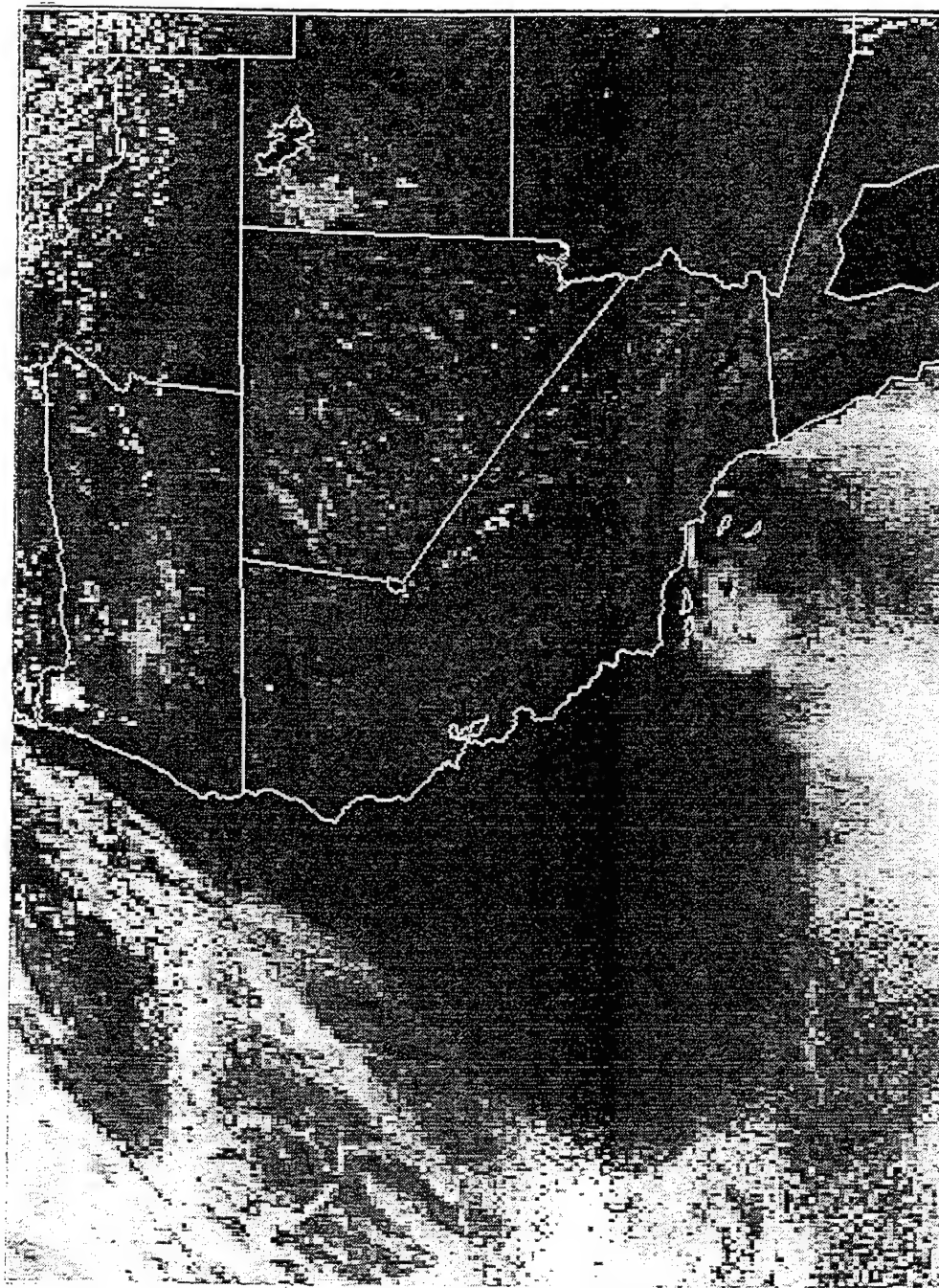
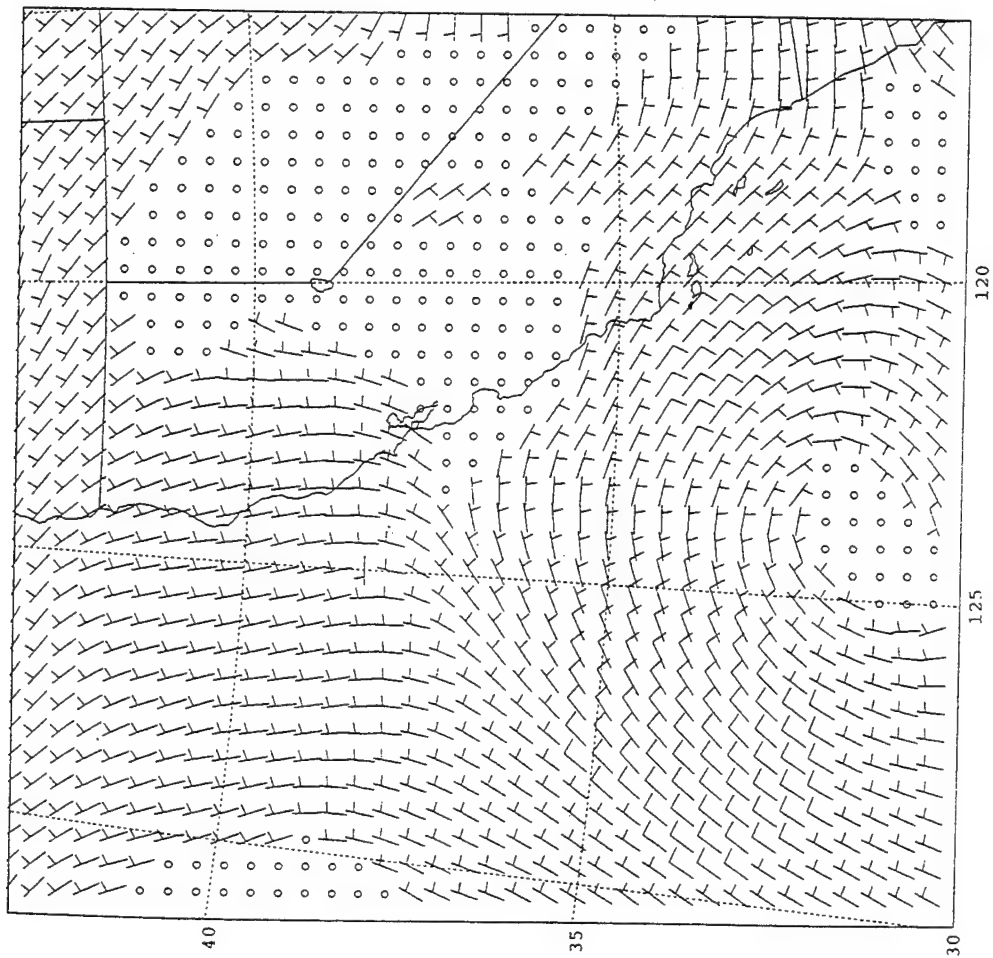
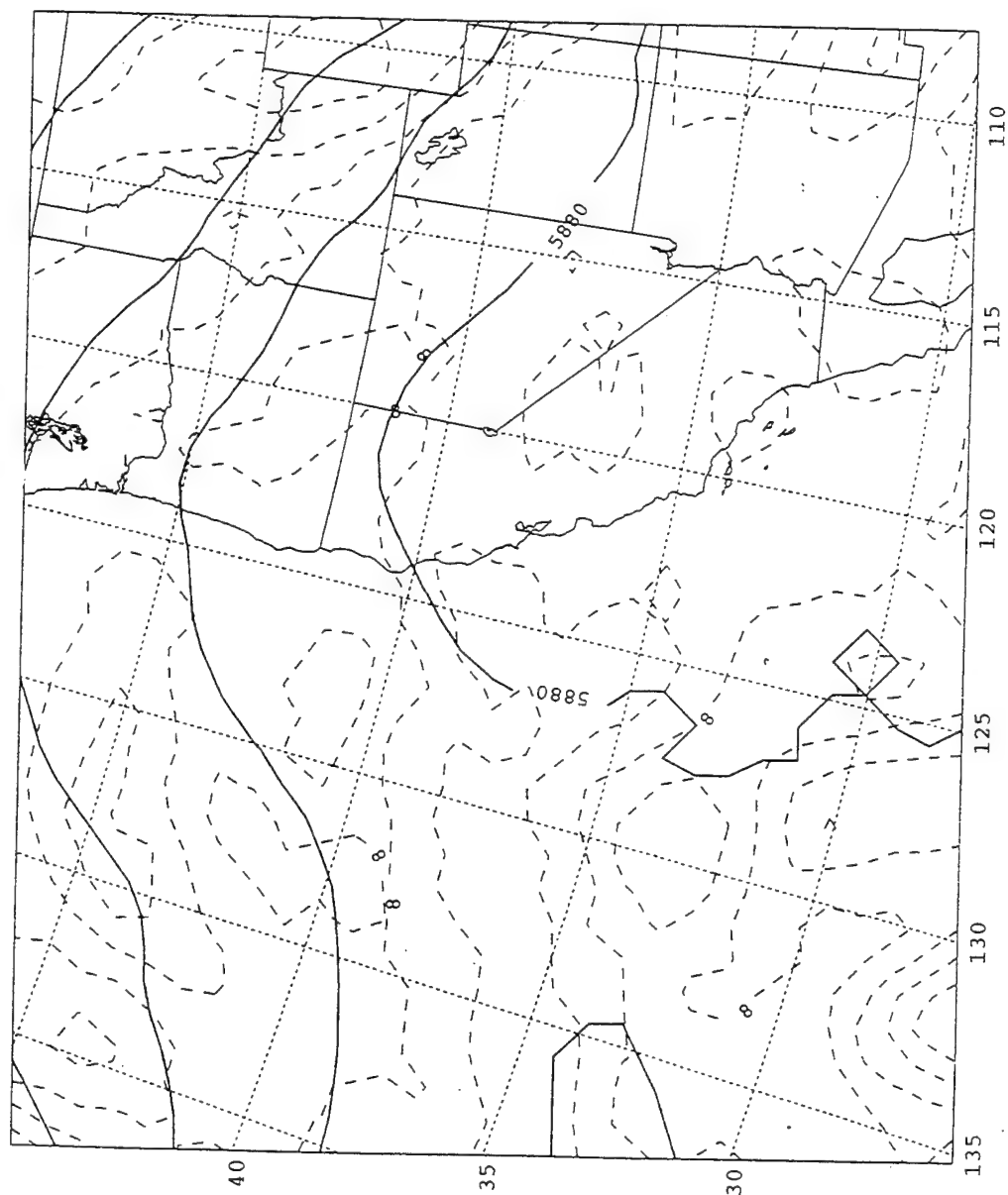


Figure 6. Visible GOES satellite image for 00UTC 10 June 1994.



**Figure 7.** 850 mb wind analysis as in Fig. 2, except for 00UTC 10 June 1994.



**Figure 8.** FTA model 500 mb geopotential height and vorticity as in Fig. 3, except for 00UTC 10 June 1994.

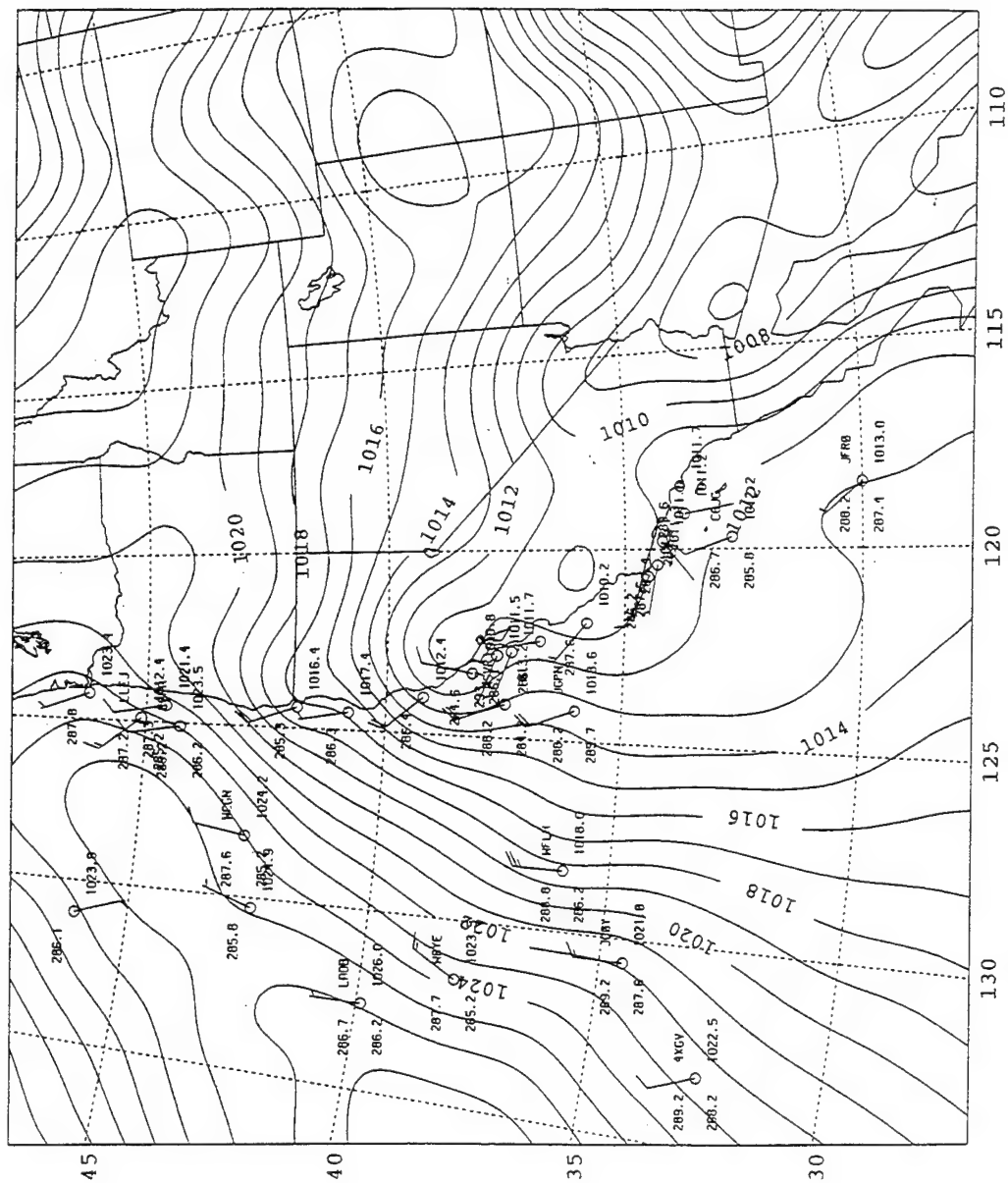
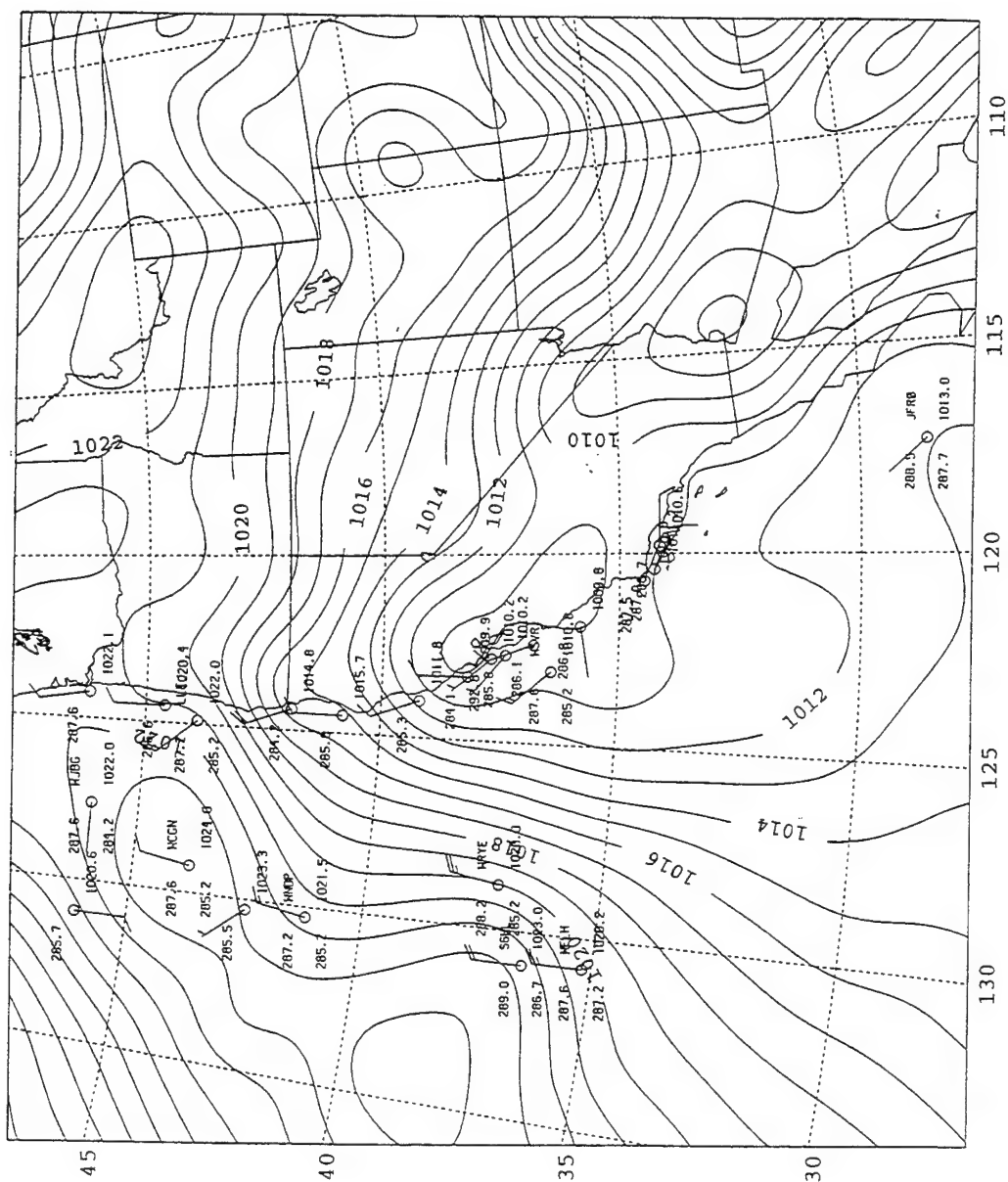


**Figure 9.** Blended SLP analysis as in Fig. 1, except for 06UTC 10 June 1994.

to generate the south to north SLP gradient. Sea-level pressure ridging is now evident across southern CA and the Channel Islands, which corresponds to the stratus building as seen in the previous visible image (Fig. 6). The surface winds in the vicinity of the Channel Islands have begun to shift to a southerly direction. In subsequent hours, the surface winds shift rapidly to southerlies near Pt. Conception.

The 12UTC 10 June SLP analysis and observations (Fig. 10) show that the surface winds have shifted to a southerly direction across the Channel Islands and in the vicinity of Pt. Conception. The SLP analysis shows that higher pressures have continued to ridge across the CB region, and the minimum SLP along the coast is near the buoy south of MRY. The thermal trough has moved farther off-shore south of MRY, and has begun to extend to the south to the west of the CB region. The 15 kt NW wind off-shore near  $36^{\circ}N$ ,  $126^{\circ}W$  indicates the seaward extent of the narrow (and coastally trapped) reversed pressure gradient. This pressure distribution supports the interpretation that the southerly winds near the coast are an ageostrophic response to the reversed along-coast pressure gradient. The 15UTC visible image (Fig. 11) shows that the stratus tongue has progressed northward along the coast nearly as far as the pressure minimum.

The 850 mb winds over most of the central coast have become light ( $<2$  kt) (Fig. 12), but maintain a slight off-shore component from north of Pt. Conception to SFO. More significantly, the cyclonic circulation at 850 mb near  $125^{\circ}W$  that was evident at 00UTC 10 June is still present and has moved slightly north and west. The corresponding SLP trough (Fig. 10) is located just east and north of this 850 mb circulation. The 500 mb





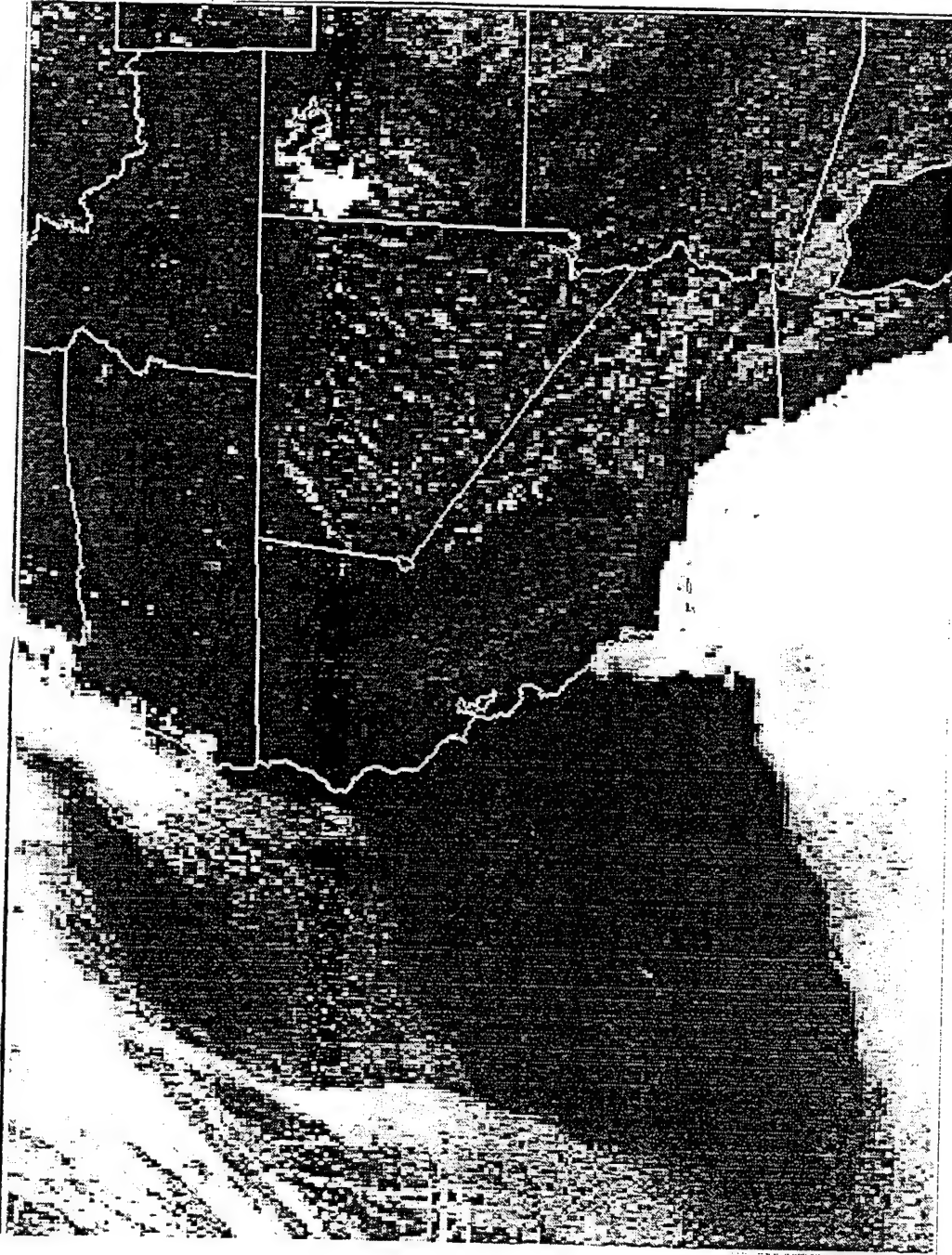
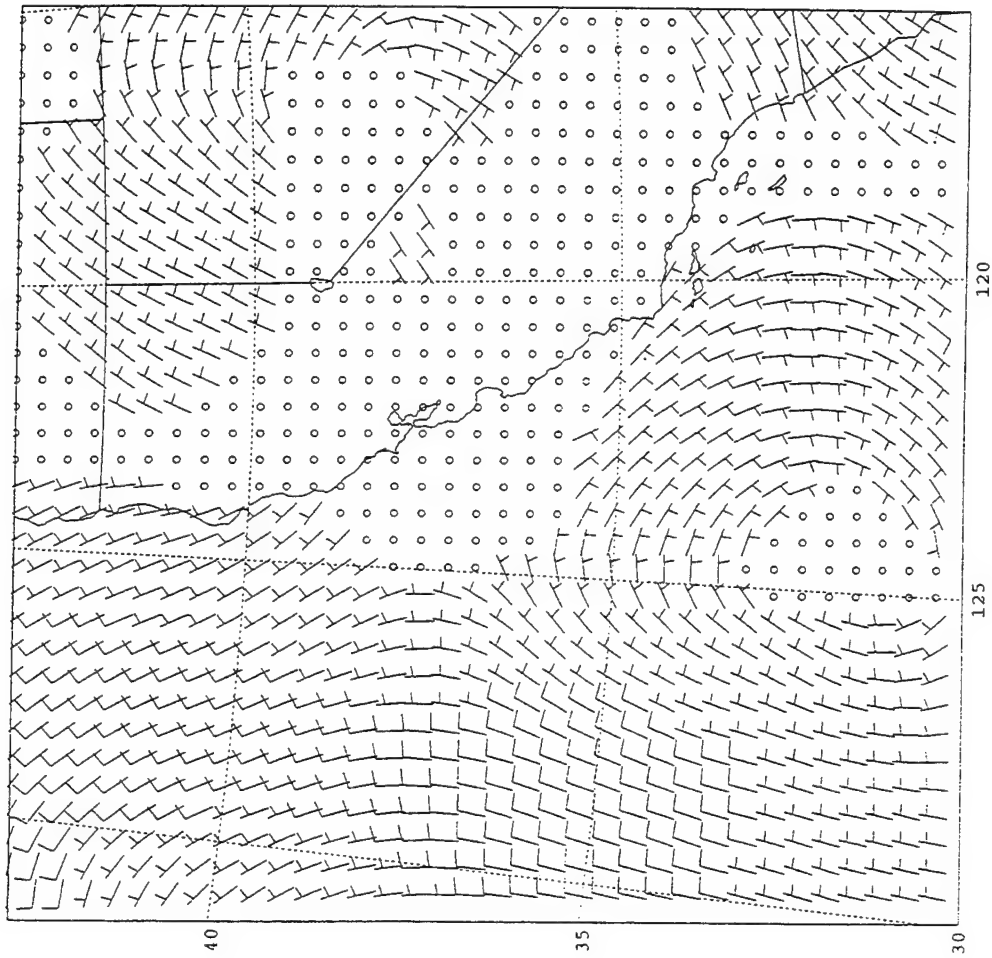


Figure 11. Visible GOES satellite image for 15 UTC 10 June 1994.



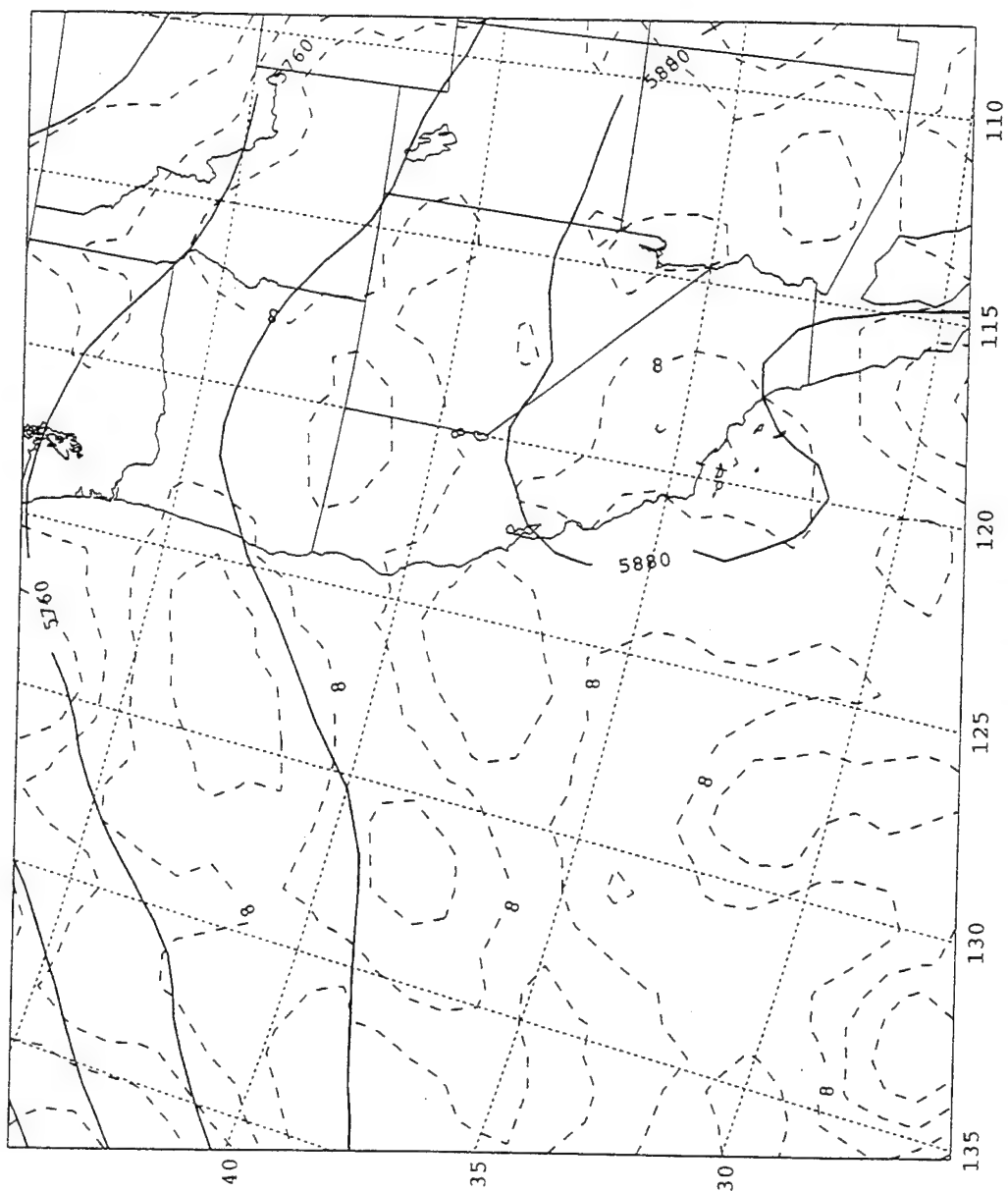
**Figure 12.** 850 mb wind analysis as in Fig. 2, except for 12UTC 10 June 1994.

height analysis (Fig. 13) shows the continued eastward progression of the ridge, particularly over the northwest United States. This pattern produced weak southerly upper (500 mb) level winds (not shown) across most of the region to the south and west of the central CA coast where the surge is occurring.

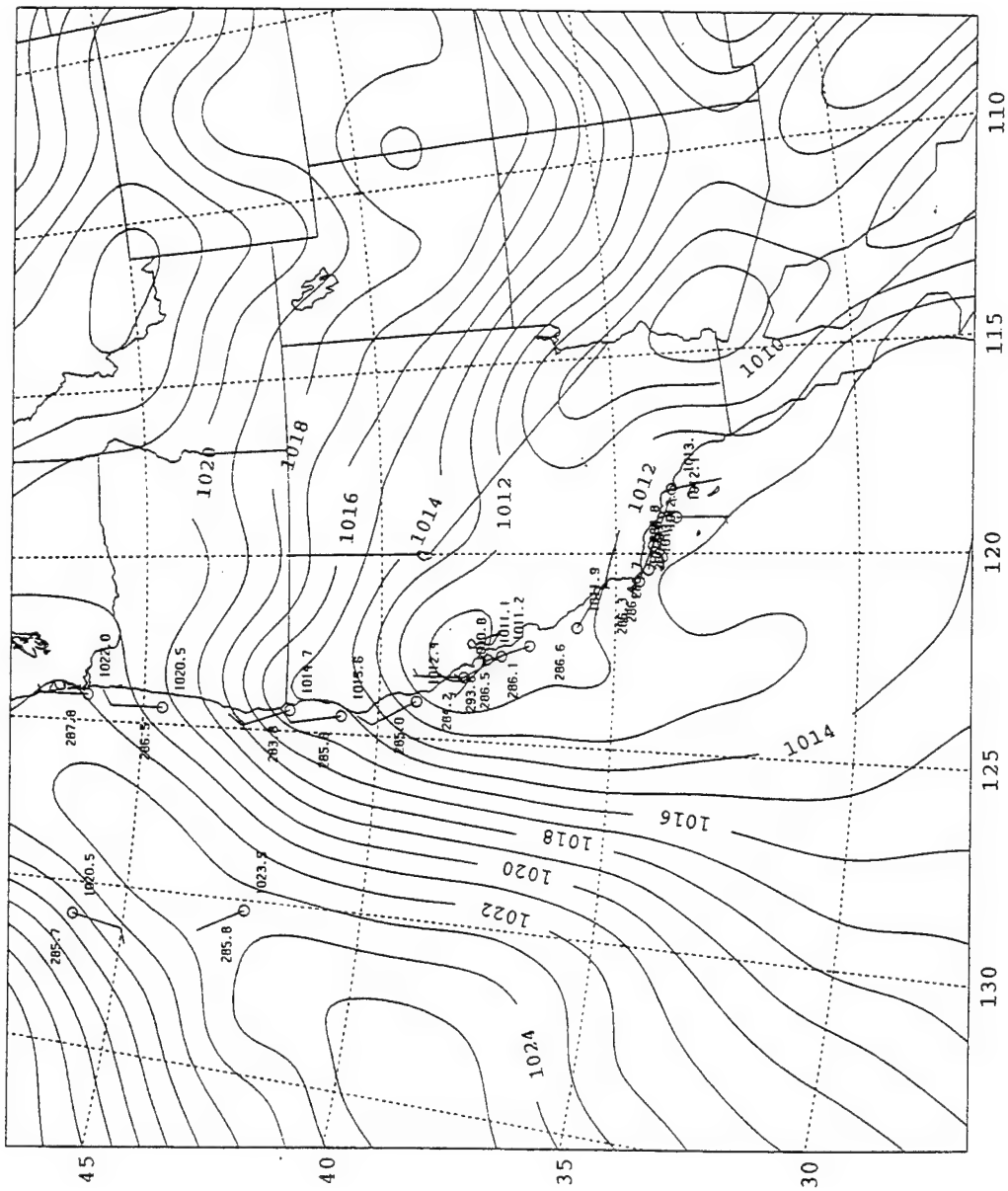
### **3. Propagation Phase**

At 15UTC 10 June, the SLP analysis and observations show southerly surface winds along the central coast to an area south of Monterey (Fig. 14). The thermal trough is centered over SFO, and the trough farther off-shore continues to extend to the south. A distinct ridge of higher pressures that now extends northward along the coast maintains the SLP gradient reversal. By 18UTC 10 June, the same general pattern in the SLP distribution is evident and is very well supported by observations (Fig. 15). These observations show that the southerly surface winds extend to the northern Monterey Bay area, which is also about the extent of the stratus as well (not shown).

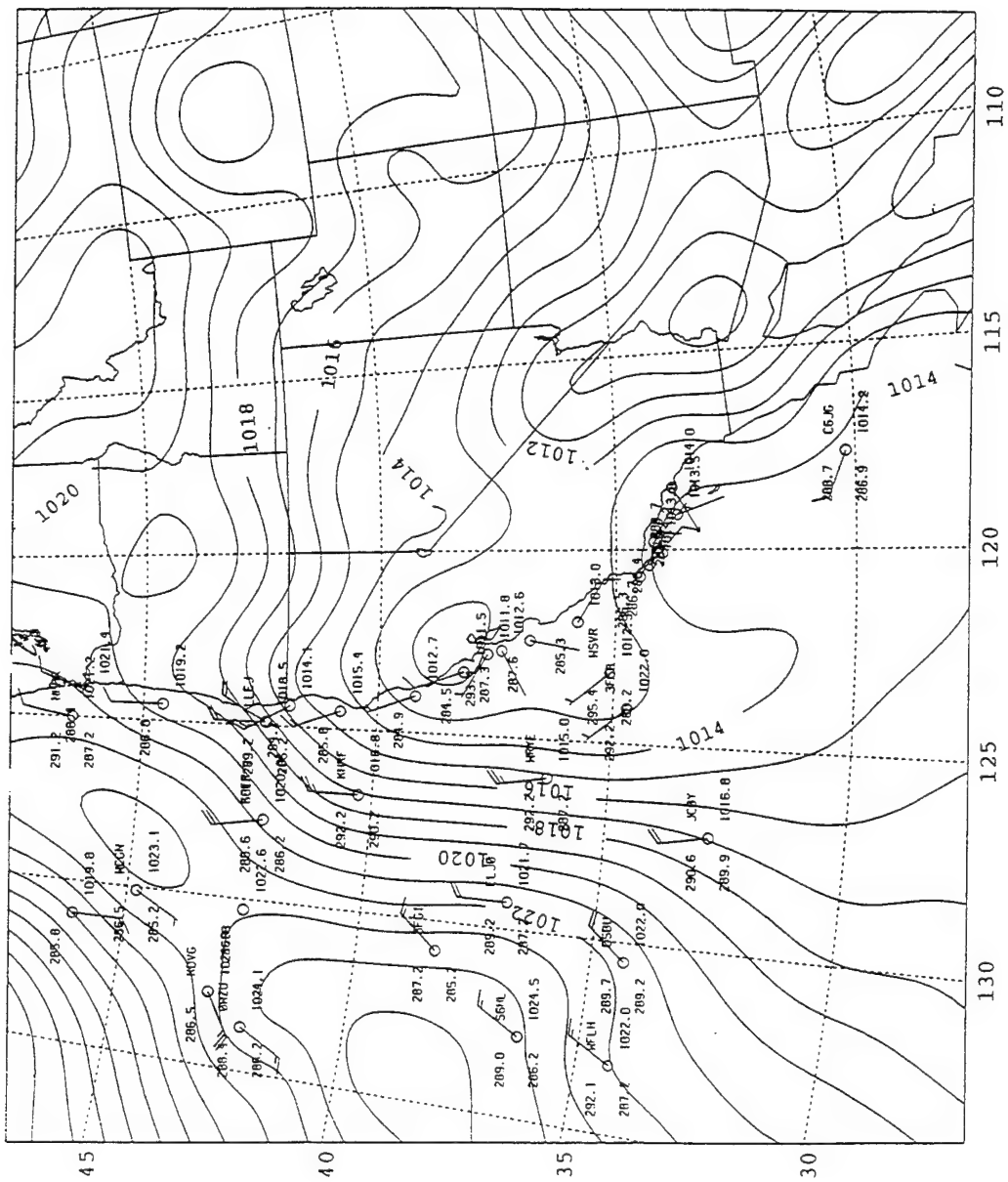
By 00UTC 11 June (Fig. 16), the SLP analysis has a closed low pressure centered near  $34^{\circ}N$ ,  $123^{\circ}W$  where there had previously been only a trough. The southerly winds along the coast from the Channel Islands to north of Monterey Bay now appear to be consistent with a simple geostrophic response to this cross-coast pressure gradient. The buoy observations show that the along-shore SLP gradient is still reversed, but the isobaric pattern also produces geostrophic southerly flow, which suggests that a trapped ageostrophic response is no longer occurring along the coast. Between 00UTC and 12UTC 11 June (Fig. 17), the low pressure center drifts northwest to near  $35^{\circ}N$ ,  $126^{\circ}W$  and the southerly winds



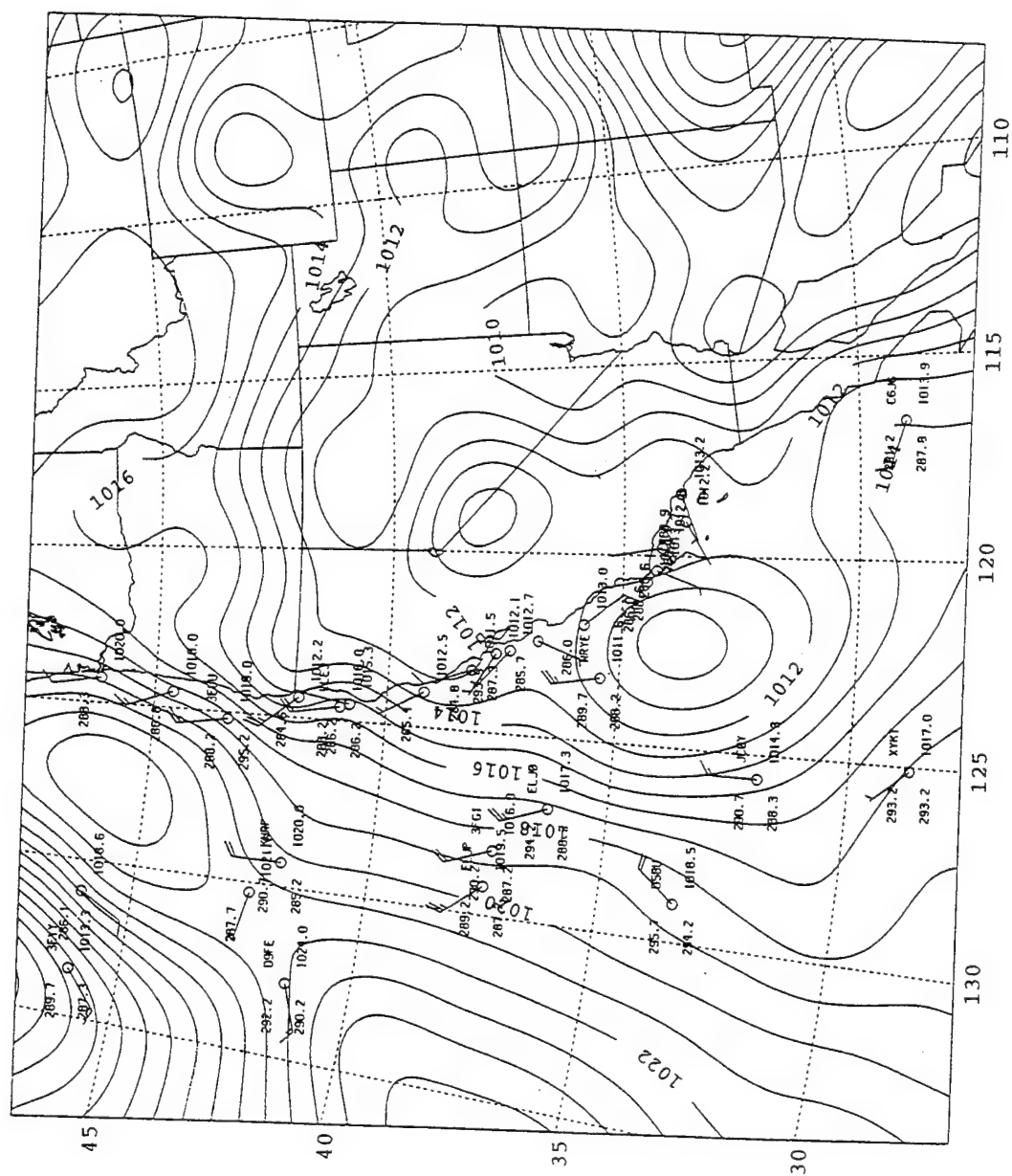
**Figure 13.** ETA model 500 mb geopotential height and vorticity as in Fig. 3, except for 12UTC 10 June 1994.



**Figure 14.** Blended SLP analysis as in Fig. 1, except for 15UTC 10 June 1994.



**Figure 15.** Blended SLP analysis as in Fig. 1, except for 18UTC 10 June 1994.



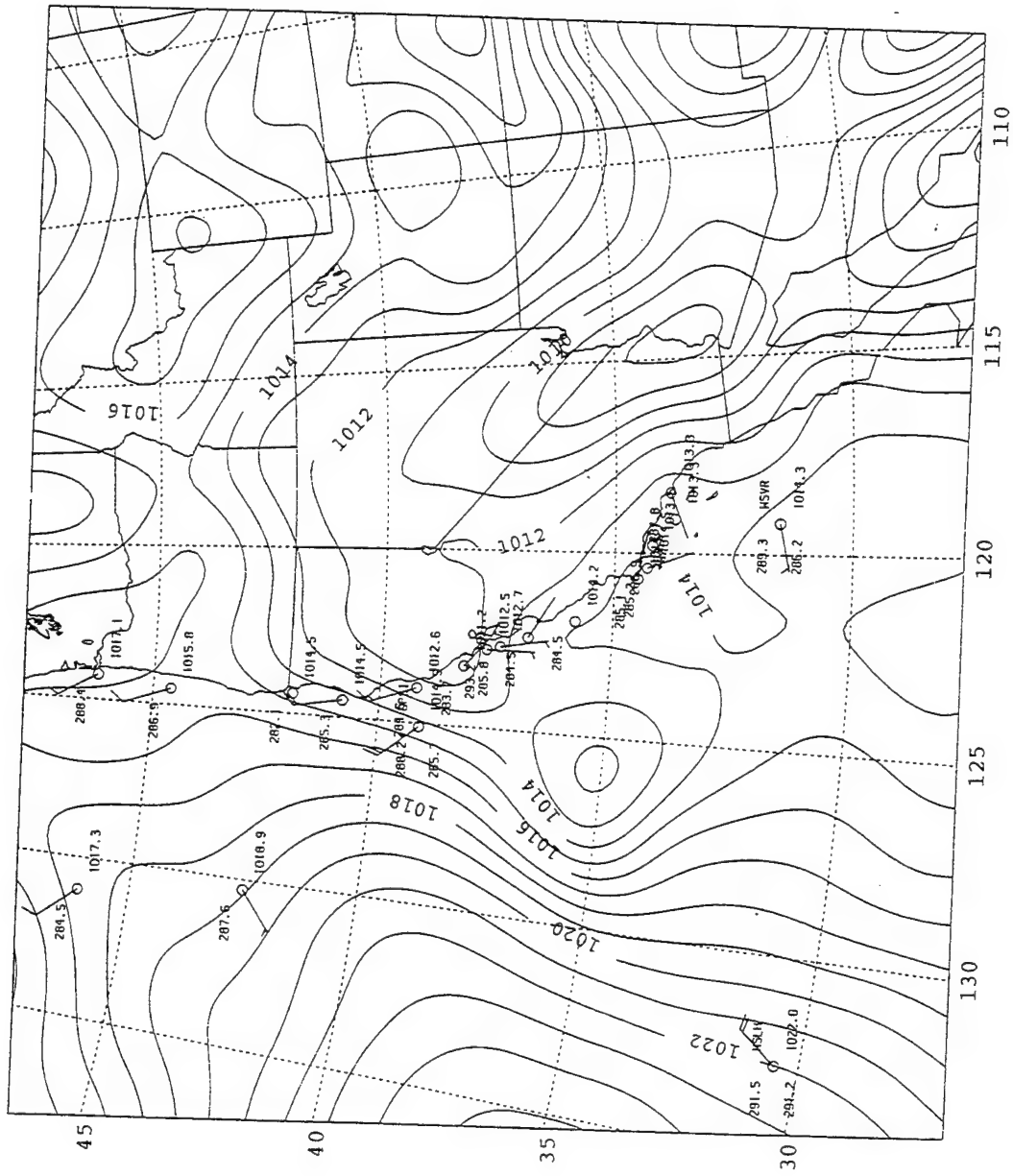


**Figure 17.** Blended SLP analysis as in Fig. 1, except for 12UTC 11 June 1994.



have progressed as far north as Pt. Arena.

The 850 mb wind analysis at 00UTC 11 June has southerly winds between the coast and  $125^{\circ}W$  from southern CA to just north of Pt. Conception (Fig. 18). Farther north along the central coast near MRY, the 850 mb winds have shifted to westerly (on-shore), which eliminates any potential lee troughing effects west of the coastal mountain range. By 12UTC 11 June (not shown), these on-shore 850 mb winds shift farther south and the off-shore cyclonic circulation is gone. The 500 mb height chart at 00UTC 11 June (Fig. 19) shows that the upper-level ridge over the Pacific Northwest has drifted slowly eastward, becoming sharper to the north and broadened at its base. The 500 mb winds (not shown) at 00UTC 11 June are light and southerly across the central CA coast similar to the flow 12 h earlier. A more pronounced southwesterly 500 mb flow is now occurring across the northern CA coast associated with the eastward shift in the ridge axis.

#### **4. Decay Phase**

By 15UTC 11 June (Fig. 20), the south to north along-shore SLP gradient has weakened substantially and the pressures along the coast are relatively equal. The thermal trough along the coast and the low pressure center near  $35^{\circ}N$ ,  $126^{\circ}W$  are both filling and shrinking in size. The southerly wind surge made it no farther than Pt. Arena, although the stratus and weak southerly winds persist to the south along the coast as indicated from the satellite image (Fig. 21) and surface observations (Fig. 20). The visible image also shows that stratus has filled in from the north along the northern CA coast in the persistent northwesterly flow. As this phase progresses, the 00UTC 12 June SLP analysis (Fig. 22)

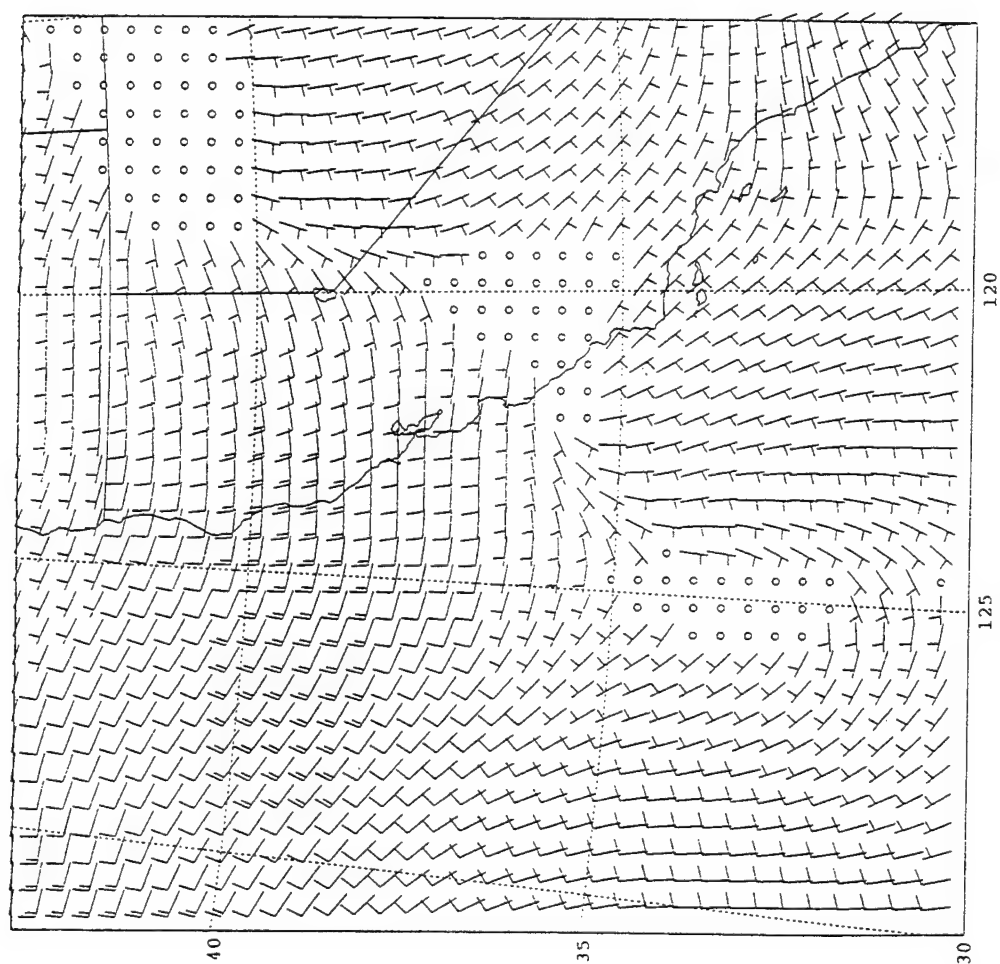


**Figure 18.** 850 mb wind analysis as in Fig. 2, except for 00UTC 11 June 1994.

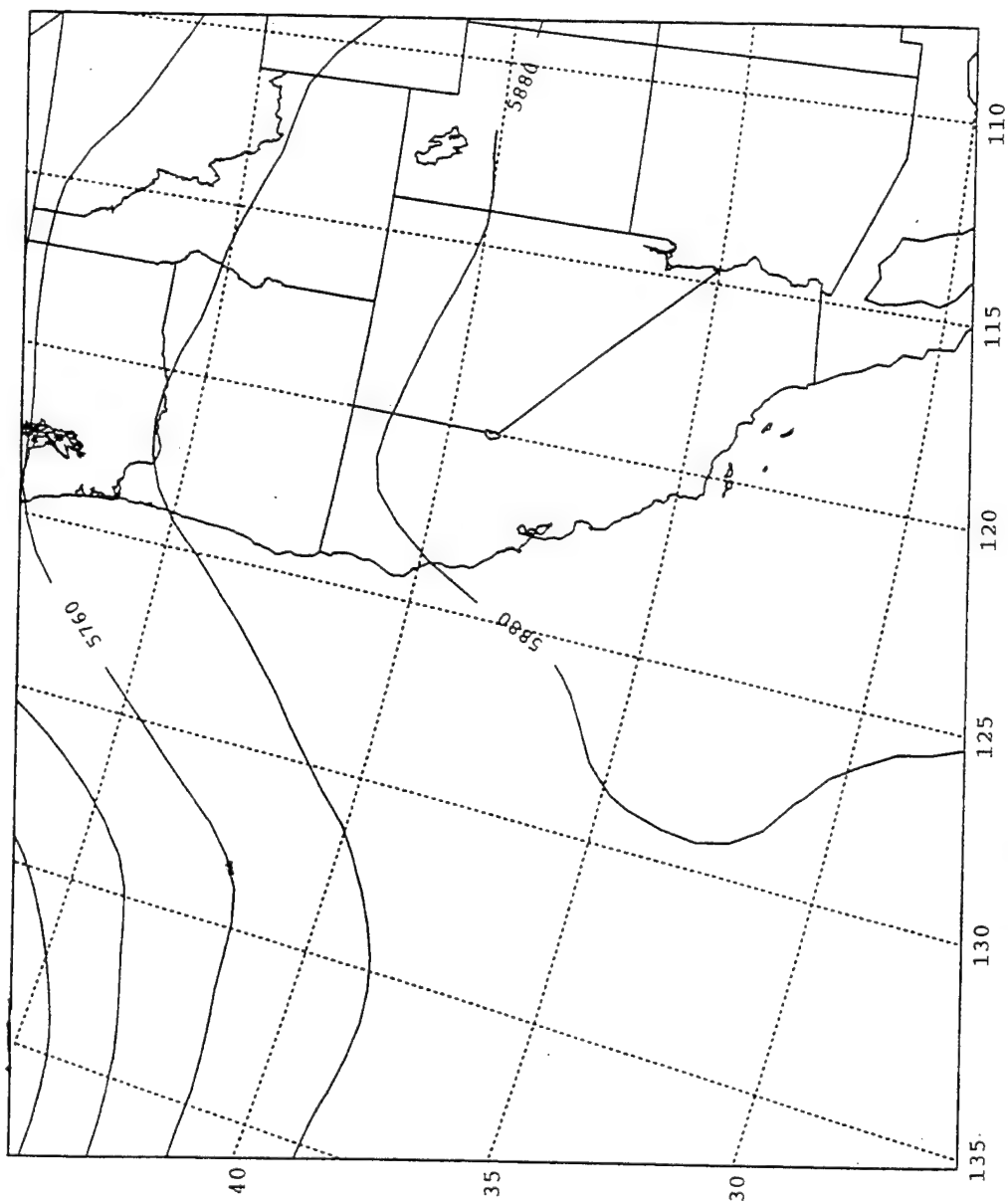


**Figure 19.** ETA model 500 mb height as in Fig. 3, except for 00UTC 11 June 1994.

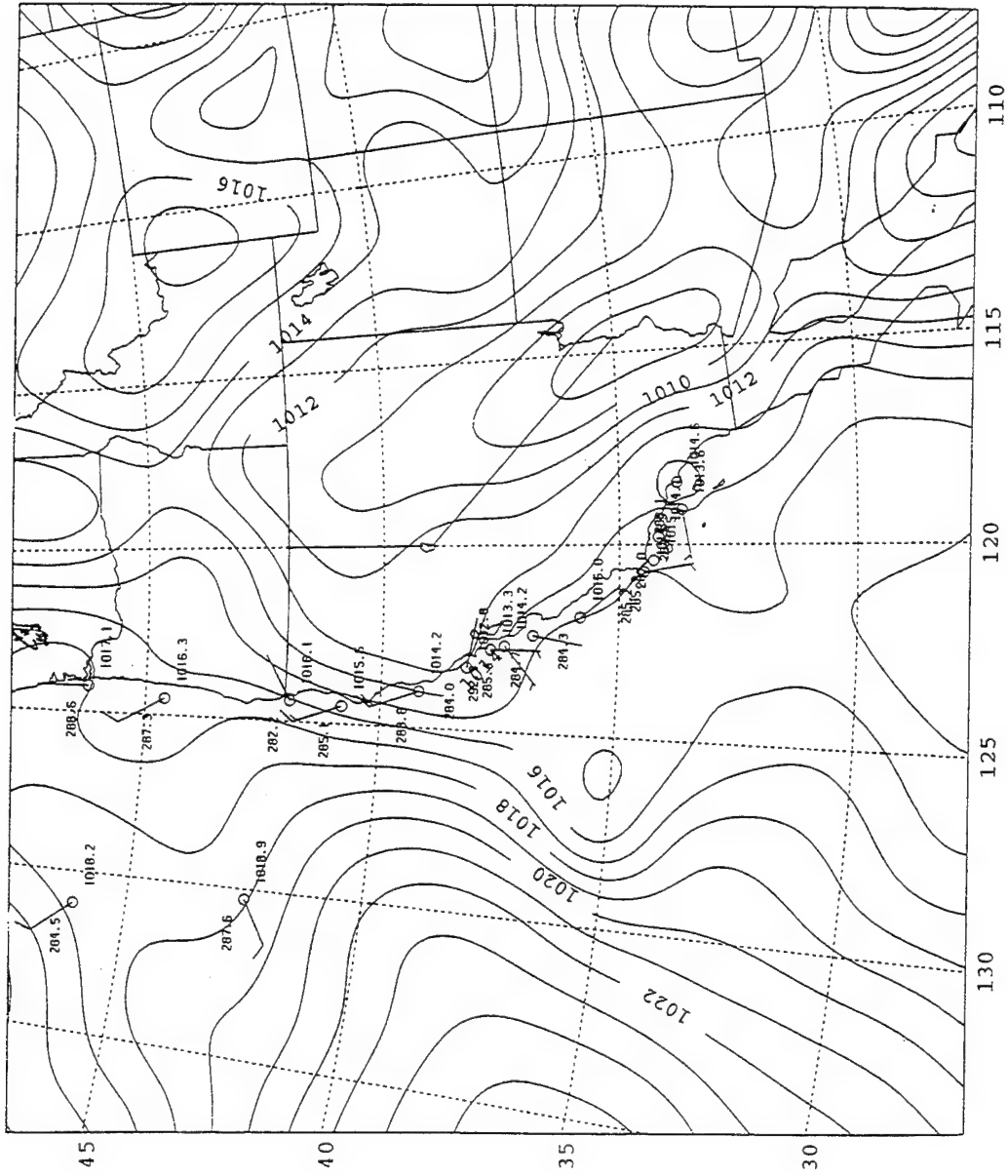


**Figure 20.** Blended SLP analysis as in Fig. 1, except for 15UTC 11 June 1994.

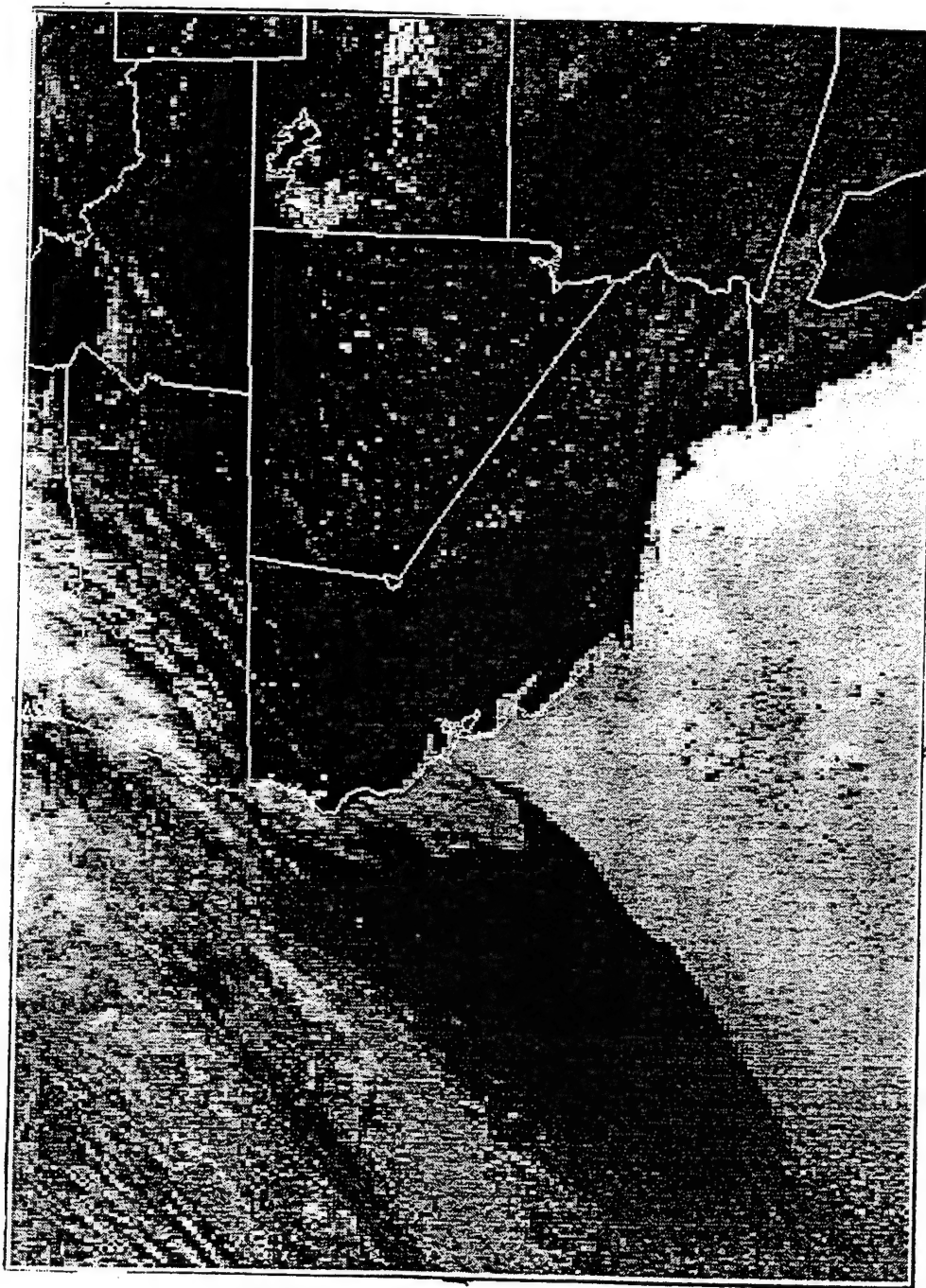
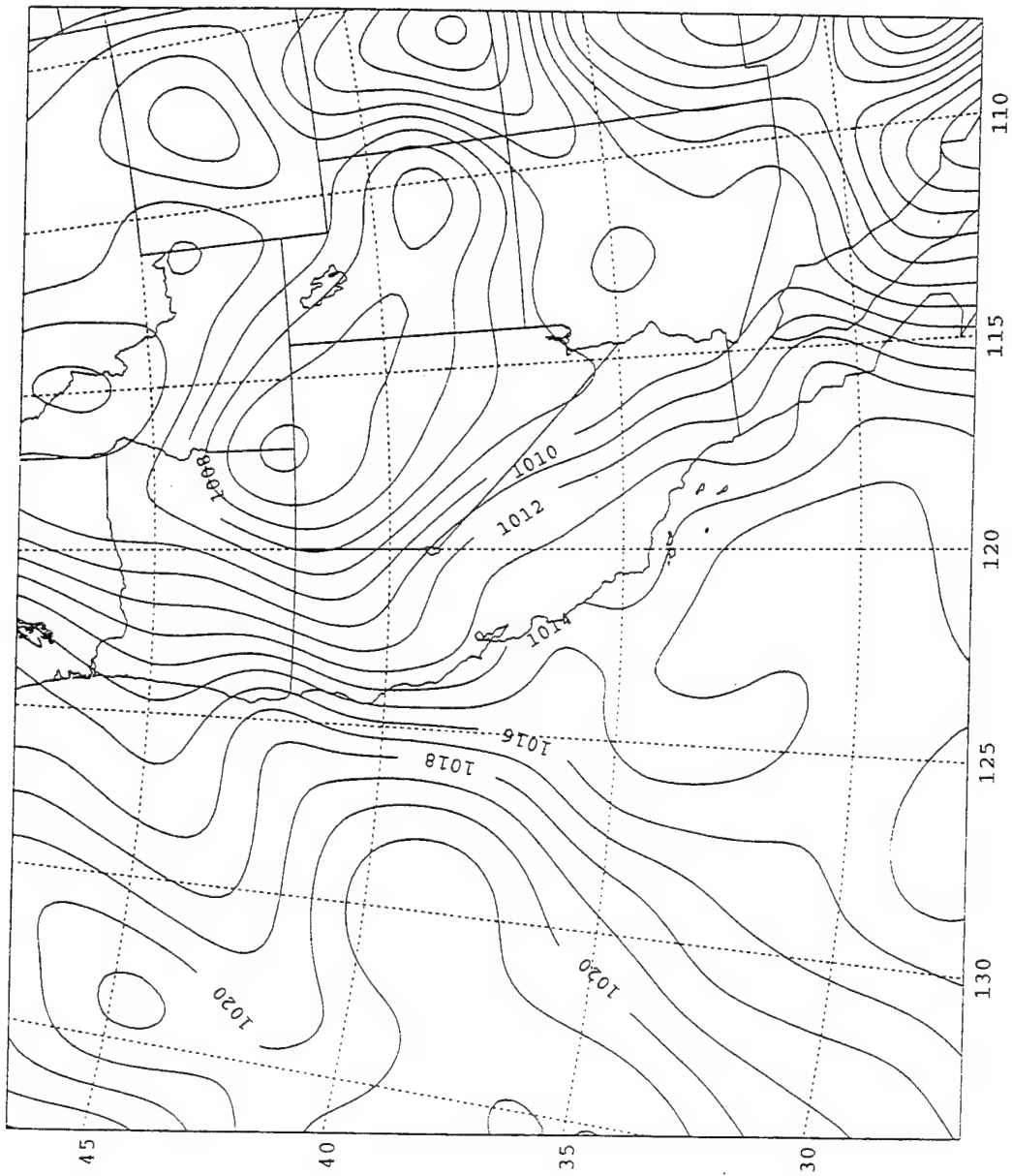


Figure 21. Visible Goes satellite image for 15UTC 11 June 1994.



**Figure 22.** Blended SLP analysis as in Fig. 1, except for 00UTC 12 June 1994.

indicates that the along-shore SLP gradient has reverted to the standard condition of higher pressures to the north and a persistent northerly coastal surface wind.

#### **5. Evolution of the Coastally Trapped Disturbance and Wind Pattern Summary**

The synoptic-scale evolution of the 10 June 1994 CTD is similar to the general evolution of the synoptic-scale structure found by Mass and Bond (1995). Surface ridging in the Pacific Northwest and the inland thermal trough are observed just prior to initiation. The surface ridging is associated with an amplifying upper-level ridge that contributes to off-shore flow at 850 mb in central California. The inland thermal trough is then extended seaward south of Monterey to produce a south to north pressure gradient along the coast south of the trough. However, several significant refinements to the evolution proposed by Mass and Bond (1995) are found in this detailed data set.

Mass and Bond (1995) suggest that the wind flow patterns in the levels above the marine boundary layer are important in producing the low-level atmospheric changes that initiate the CTD. They suggest that the off-shore synoptic-scale flow over the coastal mountains produces lee-troughing west of the coast and the mountains trap the northward ageostrophic flow along the coast. The lee-troughing is presumably responsible for the shift of the thermal trough to the coast. Although off-shore (down-slope) 850 mb winds were observed across the central California coast in the pre-initiation phase of the 10 June 1994 CTD, the thermal trough stayed well inland and only a general weakening of the along-shore pressure gradient occurred along the coast. Although this may be the effect of lee-troughing, it did not cause the along-shore SLP pressure gradient to reverse. Just prior to

initiation, the 850 mb winds shifted to southeasterly flow across the central CA coast. It is under this southeasterly 850 mb flow that an isolated SLP trough formed along a portion of the coast, which produced the pressure gradient reversal. Thus, this CTD initiation differs from that described from Mass and Bond (1995).

After the CTD had been initiated, the 850 mb winds decreased in strength along the coast and the strongest southeasterly flow shifted off-shore from central CA, which also coincided with the southward extension of lower sea-level pressures off-shore. This evolution after the initiation differs substantially from Mass and Bond (1995), who suggest that the zone of off-shore flow shifts northward with time. In this case, the 850 mb winds north of Pt. Arena remained northerly and onshore throughout the event, and finally strengthened during the decay phase. Consequently, any possible lee troughing in this region north of SFO never developed, which may have slowed or halted the CTD's advance. Although the off-shore 850 mb flow along the coast south of SFO ended shortly after initiation, the surge continued. This may have been due to the development of the coastal trough into a low pressure (SLP) center that extended southeastward off-shore. This low development provided a favorable geostrophic gradient for southerly winds along the coast.

In summary, it appears that the 10 June 1994 surge depended critically on the development of the localized coastal pressure trough, and its southward extension with time farther off-shore. The relationship between this SLP development and thermal changes, and upper-level winds will be further investigated in the next section.



## **B. SYNOPTIC-SCALE INFLUENCES ON SEA-LEVEL PRESSURE**

The evolution of SLP during a CTD event has been hypothesized as being driven by subsidence warming along the coast, which creates lee troughing on the seaward side of the coastal mountains. The lee troughing is the proposed mechanism for reversal of the along-shore SLP gradient (Mass and Bond 1995) that creates a favorable environment for the initiation and progression of the CTD. Results from the previous section suggest that subsidence warming was not the critical factor in producing the localized pressure trough along the coast during the 10 June CTD. To assess possible causes of the changes in sea-level pressures during the CTD, the 850 mb temperature changes and coastal temperature advection will be examined.

### **1. 850 MB Temperature Changes and Sea-Level Pressure Evolution**

To establish any connection between low-level temperature increases and SLP decreases, lower-level temperature changes in a series of coastal soundings (Fig. 23) were examined from 12UTC 9 June and 12UTC 10 June 1994. These soundings were taken at the Naval Postgraduate School (NPS) in Monterey CA. The shaded region indicates a temperature increase below 2500 m over the 24-h period. Above 5000 m (not shown), little temperature change was observed. This low-level temperature increase was typical among the coastal soundings from Vandenberg to Ft. Bragg preceding the event. The temperature increase was confined to the lower atmosphere below ~2000 m or 800 mb. The observed surface pressure at NPS fell by 5.3 mb over the 24-h period, which is consistent with this low-level warming.

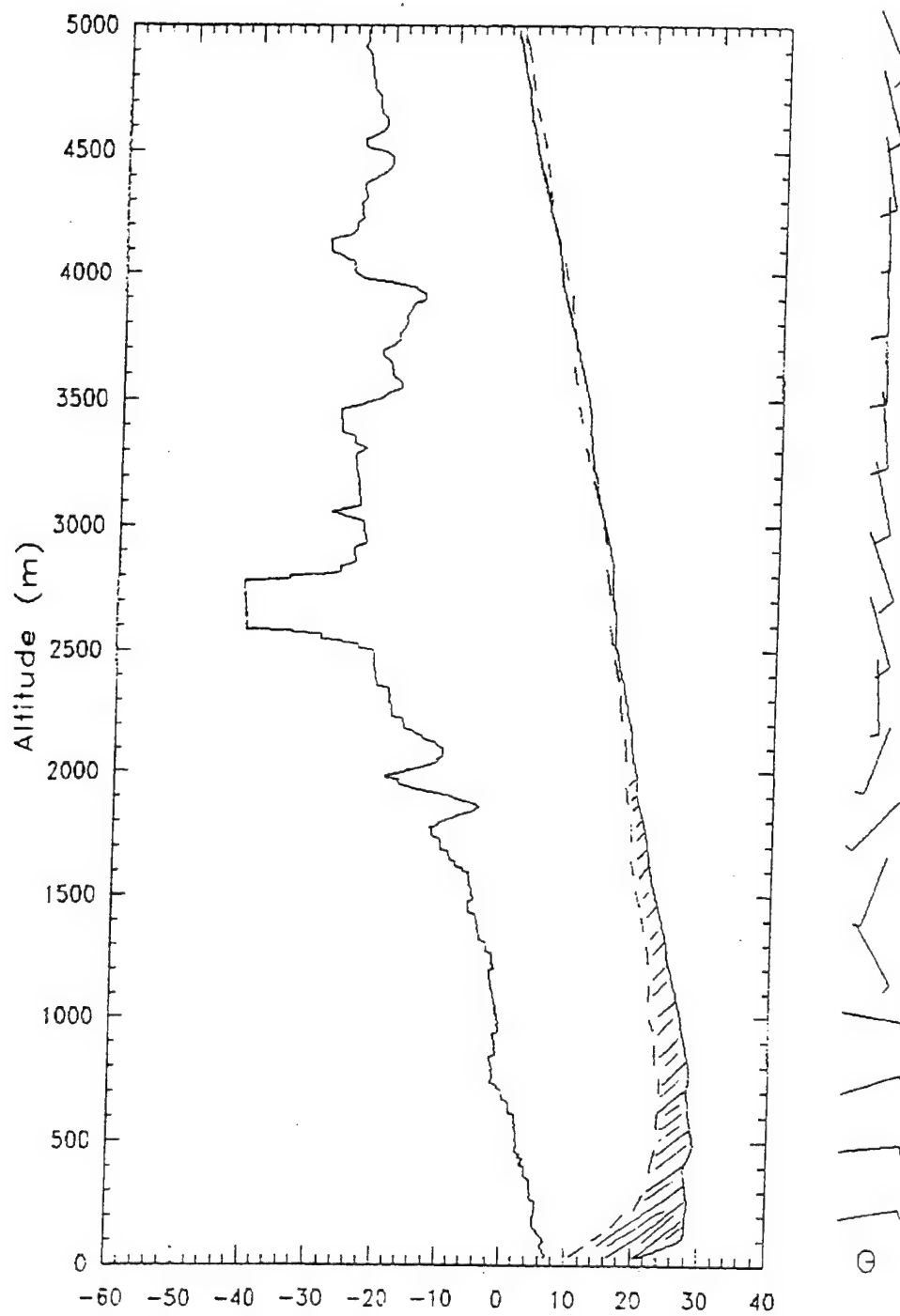


**Figure 23.** Temperature (right solid,  $^{\circ}C$ ) and dew point (left solid,  $^{\circ}C$ ) profiles at N. P. S. for 12UTC 10 June. Dashed line is temperature ( $^{\circ}C$ ) for 12UTC 9 June 1994. Shaded region is temperature increase.

To calculate the relative contribution of low-level temperature change to SLP changes, the soundings on 9 June and 10 June 1994 from NPS were compared. From examination of the data we found that the 800 mb height decreased (i.e., contribution from temperature changes above 800 mb) 17.3 m over the 24-h period, which accounted for 1.9 mb of the SLP change, and virtual temperature changes below 800 mb accounted for 3.6 mb (70%) of the SLP change. This calculation for NPS suggests that there is a strong correspondence between low-level temperature changes and SLP changes along the coast in this case.

Other soundings along the central CA coast displayed similar trends in the rise of lower-level temperatures and in SLP falls during the event, which suggests that 850 mb temperature change will be indicative of SLP changes. 850 mb was chosen over 925 mb for examination because the latter analysis will include low-level temperature advection, and 925 mb would not be available over portions of California and the southwestern states because of the steeply sloping topography in this region. Charts of SLP and 850 mb temperature change were generated for 24-h periods throughout the event. The 24-h period was chosen to eliminate diurnal effects in the changes of temperature. As indicated above, the relationship between 850 mb temperature change and SLP change does not take into account the height changes aloft (say at 800 mb) associated with the large-scale synoptic circulation. The aim of this diagnosis is simply to identify regions, specifically along the CA coast, that are characterized by low-level warming that could account for a significant portion of any surface pressure decreases.

Temperatures at 850 mb for the pre-initiation period 00UTC 9 June to 00UTC 10 June (Fig. 24) are increasing across the western states, and extending seaward from central CA. Temperature increases of  $2^{\circ}$  to  $4^{\circ}K$  are indicated from SFO through the CB region and a local maximum of temperature rises extends from the CB region seaward to near  $32^{\circ}N$ ,  $125^{\circ}W$ . The SLPs for the corresponding period (Fig. 25) are falling in generally the same broad areas. That is, the western states have SLP decreases, as does the entire coast of CA. A local area of SLP falls that extends southwest (seaward) from SFO roughly corresponds to the lobe of 850 mb temperature increases off the CB region.

During the initiation phase, 12UTC 9 June to 12UTC 10 June, warming at 850 mb occurs across nearly the entire region (Fig. 26). Specific areas of local maxima include the northern CA coastal region and the Pacific Northwest. A prominent lobe of increasing temperatures extends south along  $128^{\circ}W$  from the maximum off northern CA. The only region of decreasing 850 mb temperatures was south of the CB region, which is the region in which the stratus build up occurred (Fig. 6). The corresponding SLP change (Fig. 27) has a localized area of pressure decrease corresponding very well with the region of temperature increase off northern CA, and a second area corresponding to the trough of increasing temperatures extending south from northern CA. Small pressure increases are found south of the CB region, which roughly corresponds to the area of decreasing 850 mb temperatures. The general trends for 850 mb temperature changes and SLP changes correspond quite well.

The third period (00UTC 10 June to 00UTC 11 June) for which 850 mb temperature

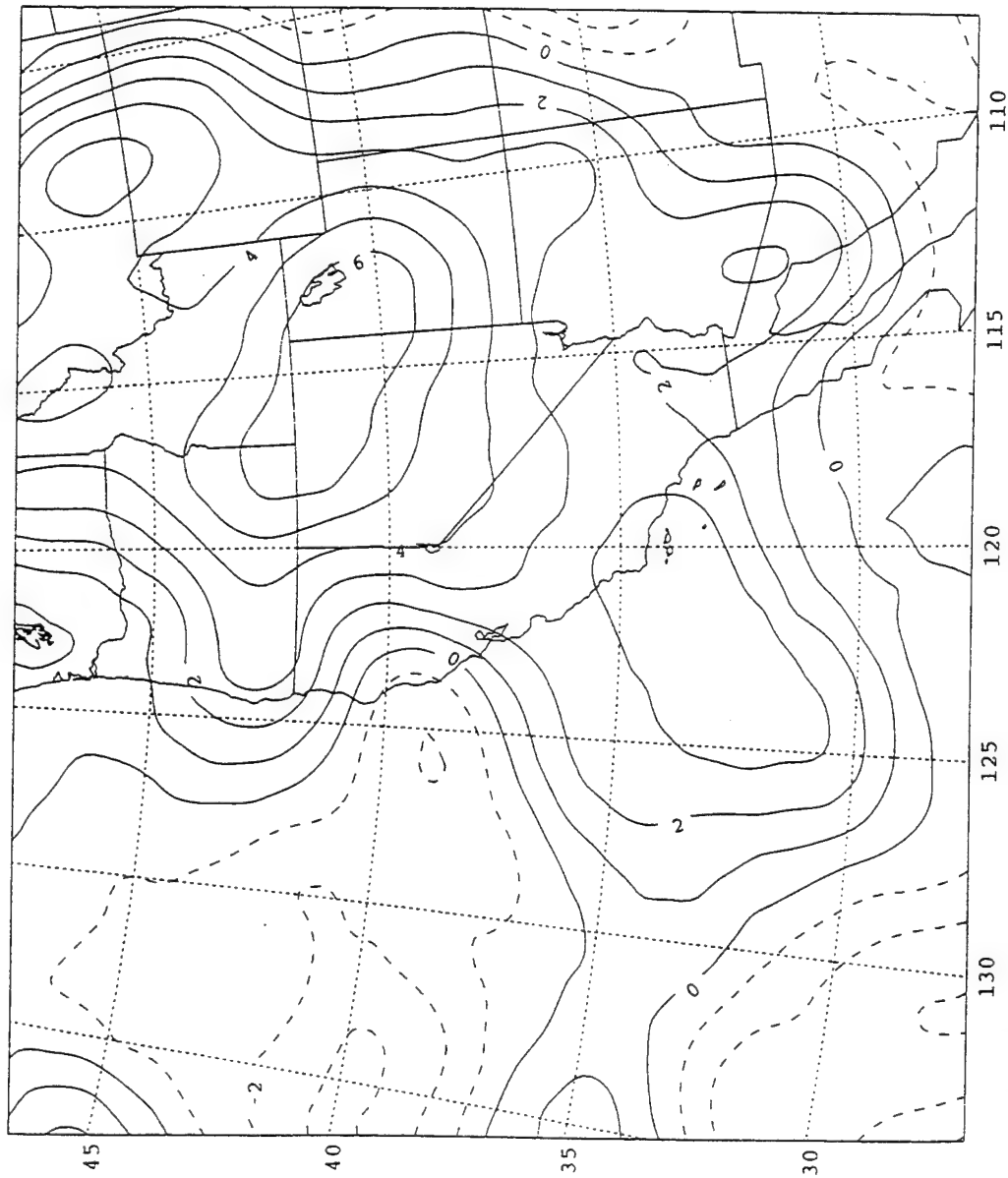


**Figure 24.** 850 mb temperature change ( $^{\circ}\text{K}$ ) from 00UTC 9 June to 00UTC 10 June 1994. Warming (cooling) indicated by solid (dashed) isotherms.

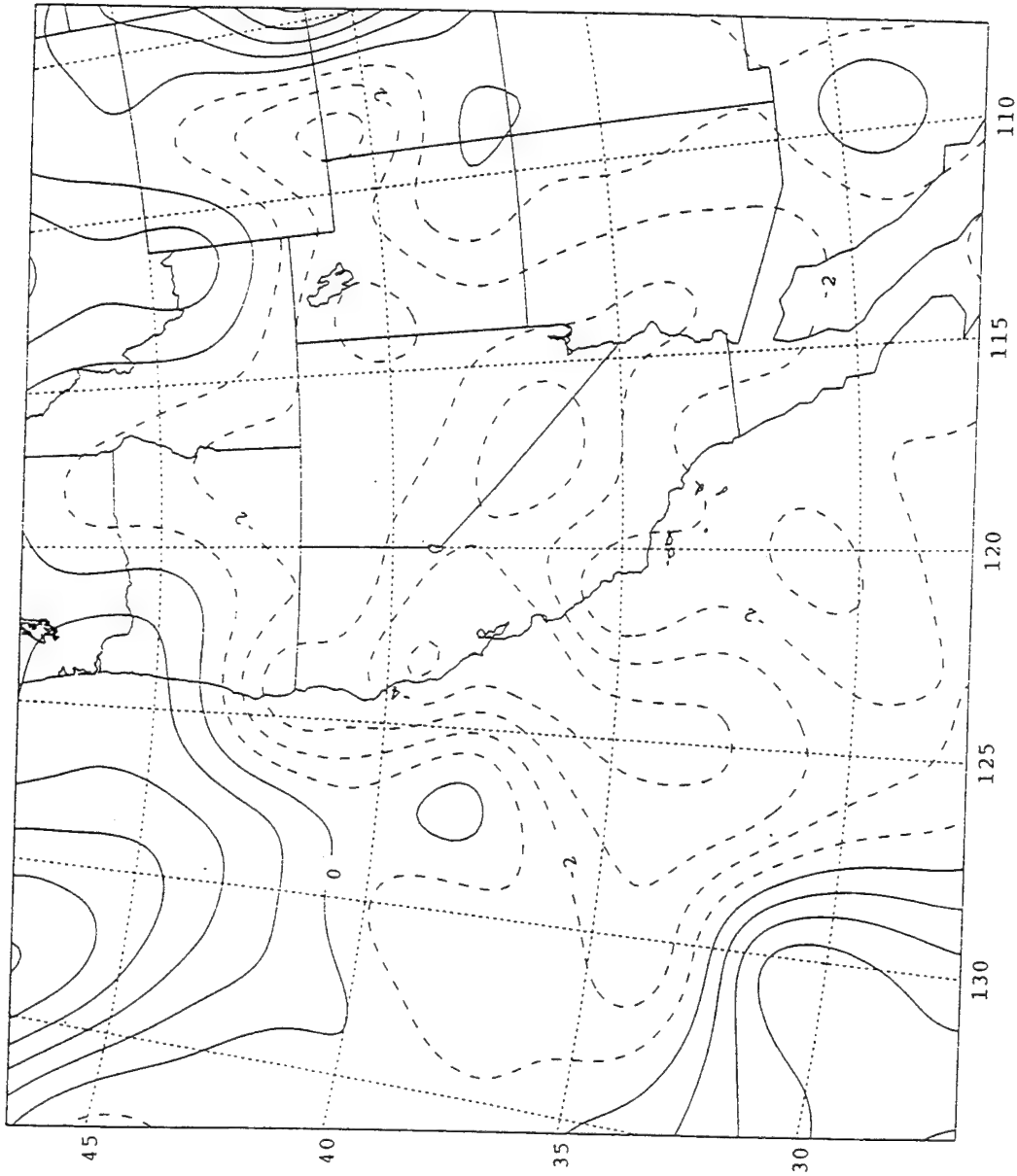


**Figure 25.** Blended SLP change (mb) from 00UTC 9 June to 00UTC 10 June 1994, with rises (falls) indicated by solid (dashed) isobars.

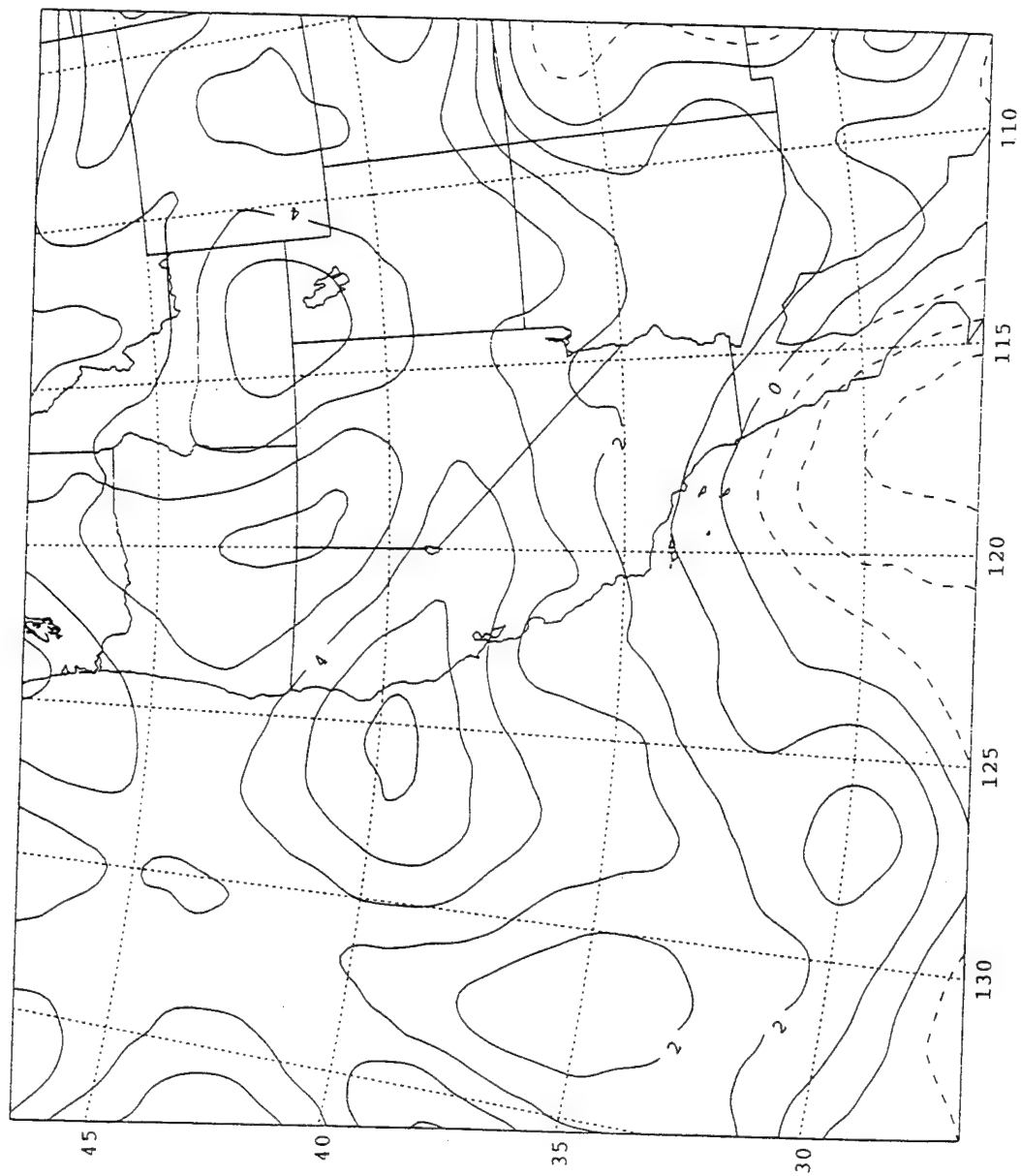


**Figure 26.** 850 mb temperature change as in fig. 24, except from 12UTC 9 June to 12UTC 10 June 1994.

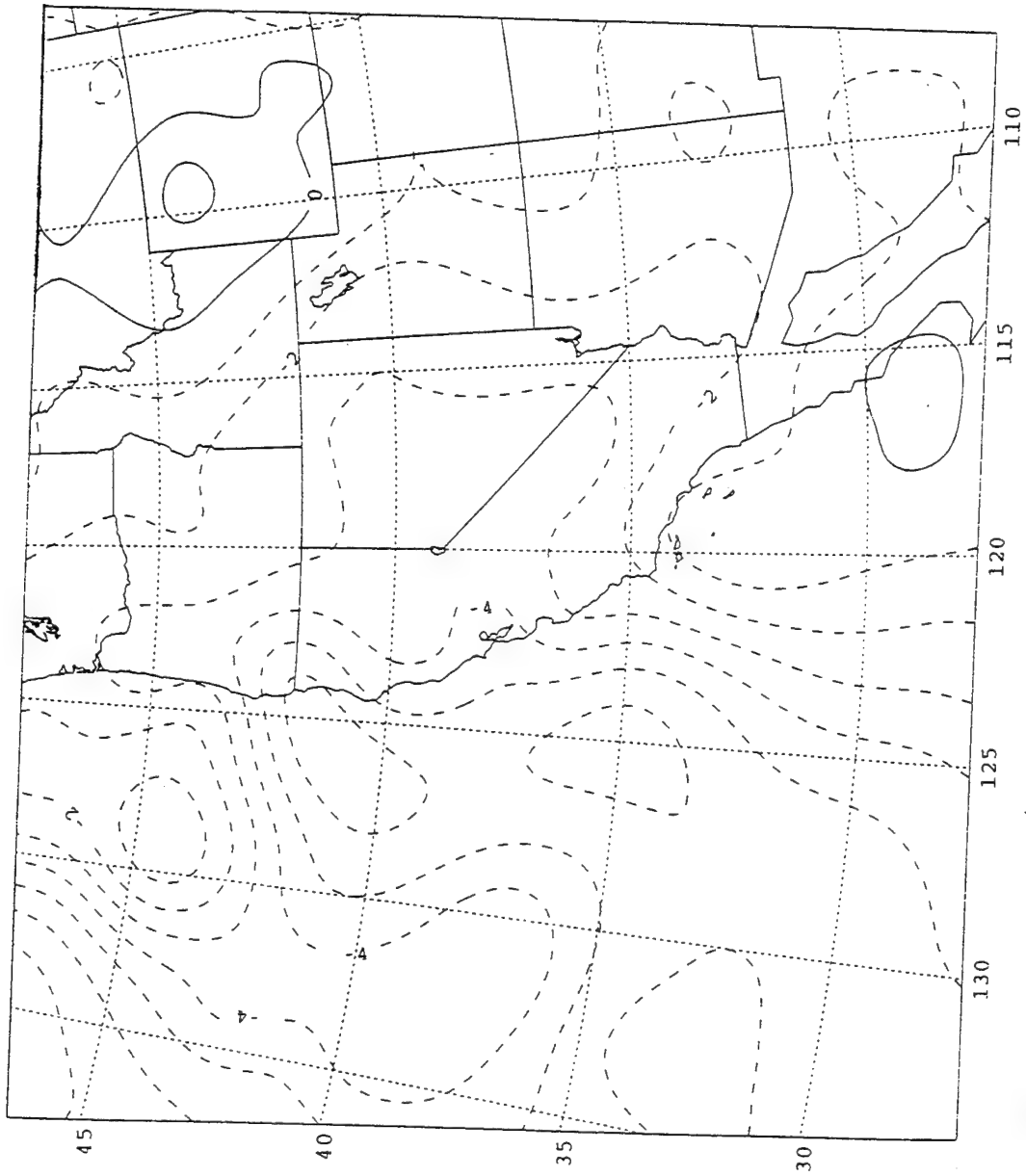


**Figure 27.** Blended SLP change as in Fig. 25, except from 12UTC 9 June to 12UTC 10 June 1994.



(Fig. 28) and SLP (Fig. 29) change plots were constructed has a good correspondence as well. Temperature increases are centered off northern CA, and general temperature rises extend southward and eastward from northern CA. An interesting feature is an area of small temperature decreases extending northward along the central CA coast from south of the CB region. This area corresponds well to the propagation of the stratus and fog (Fig. 11) along with the CTD. SLP decreases (Fig. 29) correspond quite well with the general regions of 850 mb temperature increases. Specifically, a localized region of SLP decreases off northern CA corresponds to the region of 850 mb temperature increases. An area that does not seem to correspond very well is off Pt. Conception where zero temperature changes are found, but SLP decreases are strongly centered off-shore. This area corresponds to the off-shore trough and the development of the low pressure center, which suggests other dynamic forcing is contributing in that region during the time period.

It is quite apparent from several areas with little or no correspondence between the SLP and 850 mb temperature changes that changes through a deeper column are affecting the SLP changes. Most of these discrepancies are over land areas where large-scale circulations in the upper levels (forcing vertical motions), horizontal thermal advection, or some combination of both may be influencing the SLP changes. However, the coastal soundings in CA indicate that the 850 mb temperature change accounts for most of the observed pressure changes along the coast.

## **2. Thermal Advection and 850 MB Temperatures**

Based on the thermodynamic energy equation, temperature changes occur by three

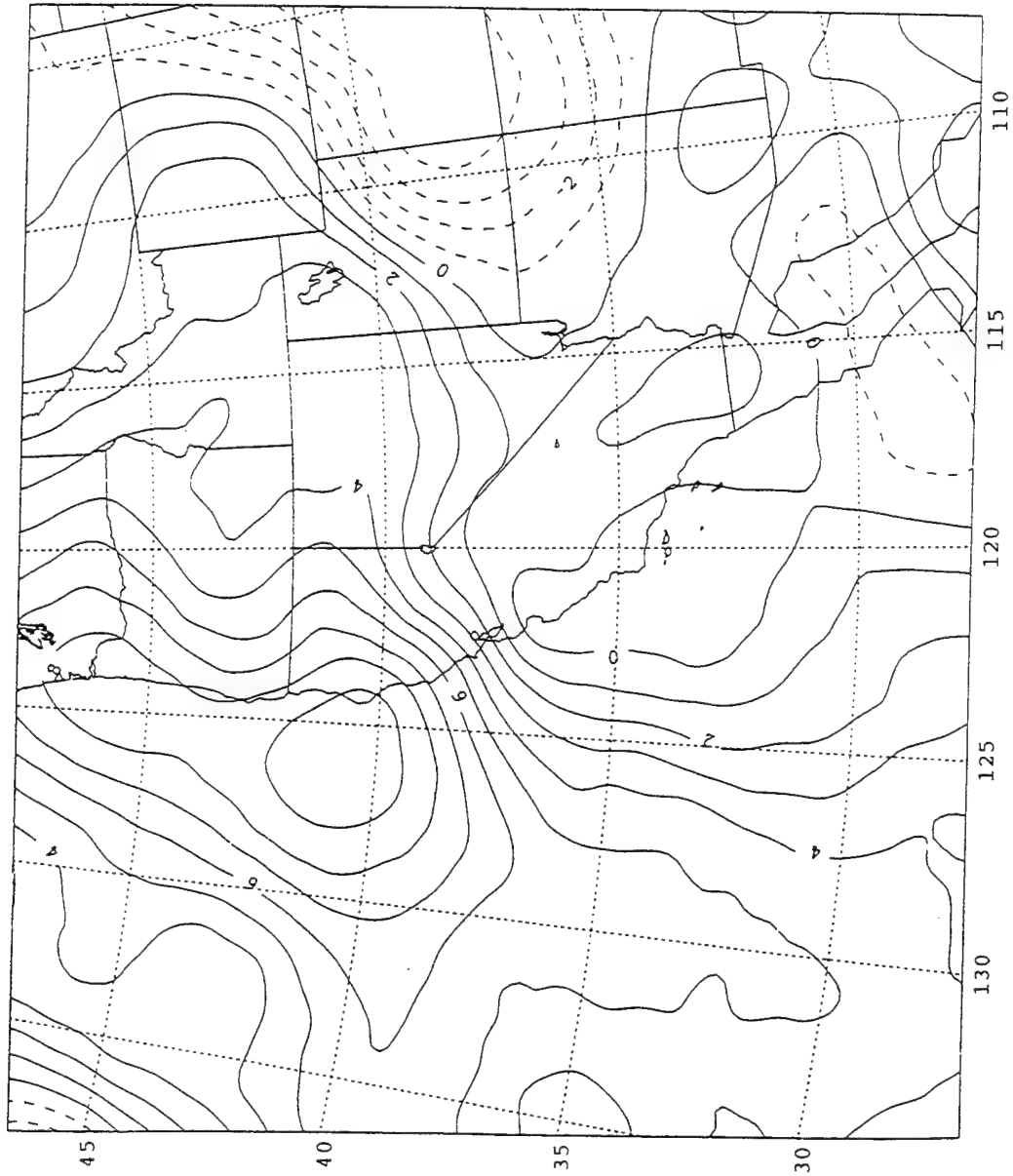


**Figure 28.** 850 mb temperature change as in Fig. 24, except from 00UTC 10 June to 00UTC 11 June 1994.

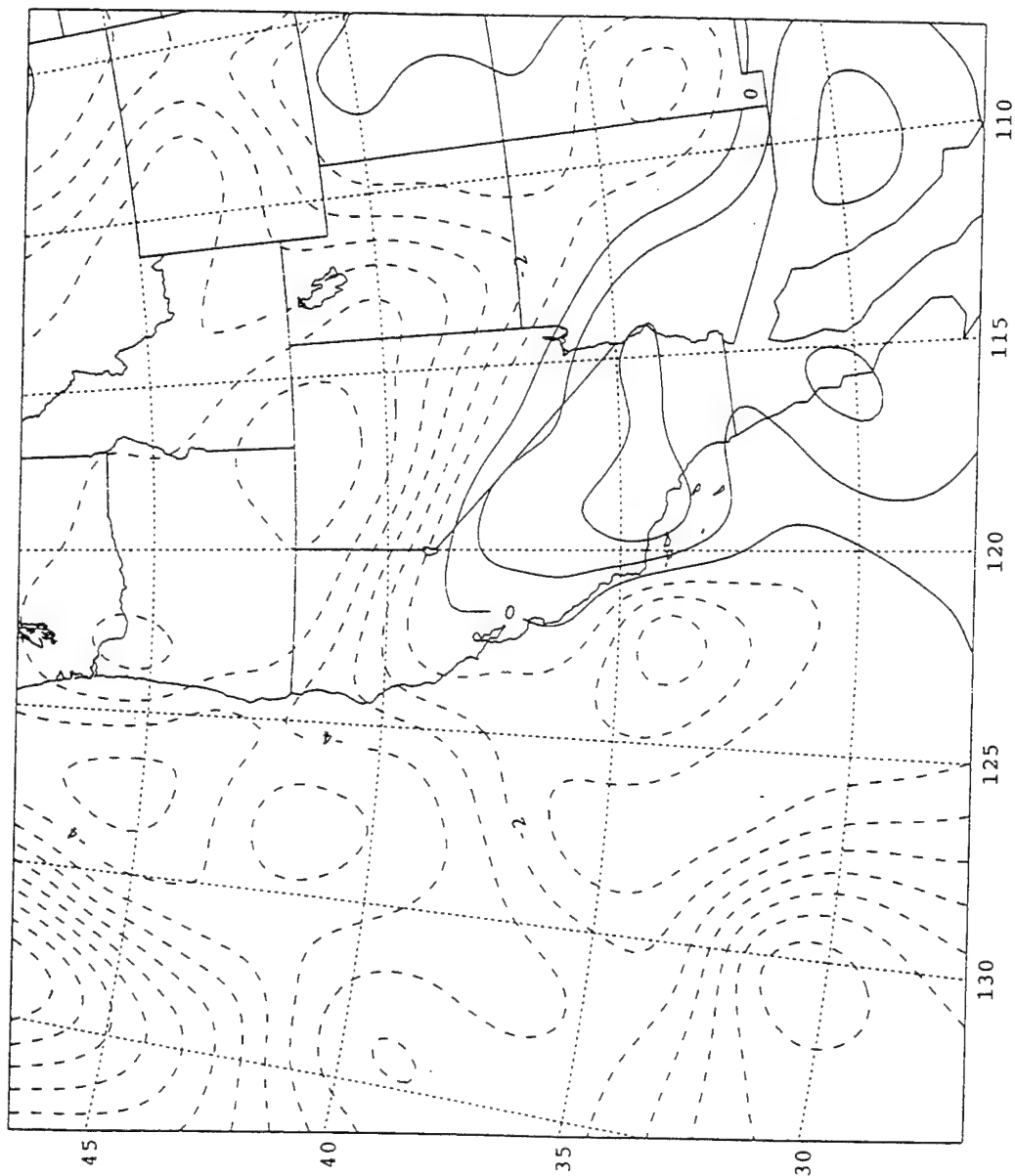
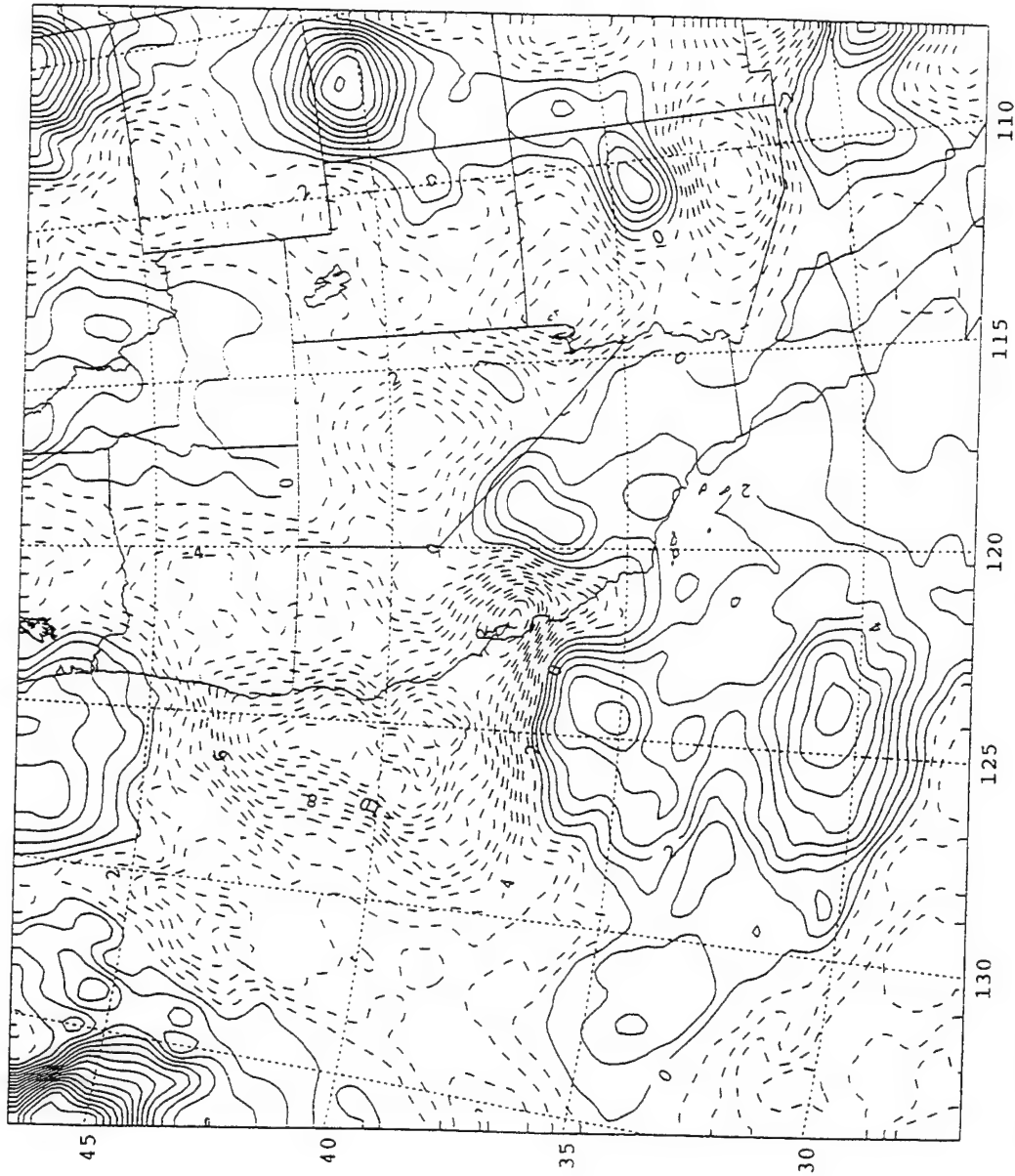


Figure 29. Blended SLP change as in Fig. 25, except from 00UTC 10 June to 00UTC 11 June 1994.

processes: horizontal thermal advection, vertical motion, and diabatic heating. The diabatic heating is probably small in the clear air, and is largely diurnal in nature over land. Vertical motions were not analyzed in this study. Consequently, thermal advection will be examined as a possible cause of the temperature change at 850 mb. The adiabatic warming and cooling and diabatic heating effects will then be inferred from any temperature change not explained by horizontal advection.

From 00UTC 9 June to 00UTC 10 June (Fig. 24), 850 mb temperature rises were indicated along the coast and in a lobe of warming extending seaward (southwest) from the central CA coast. The intermediate 850 mb thermal advection for 12UTC 9 June (Fig. 30) has a broad area of positive advection (warming) south of Pt. Conception, which covers the majority of the lobe of warming on the temperature change chart (Fig. 24). Over much of the remaining regions, and especially over northern and much of central CA and the western states, large values of cold air advection are occurring in regions of temperature increases. Thermal advection clearly does not explain the rising temperatures off northern CA. Subsidence must be the cause of the warming, which indicates lee troughing is a possible explanation. However, the 850 mb winds at 12UTC 9 June (Fig. 2) and 00UTC 10 June (Fig. 7) indicate northerly on-shore flow prevails from Oregon to near SFO, rather than the off-shore flow required to generate a lee trough. The 700 mb winds (not shown) indicate the same weak northerly flow across the region. Thus, the warming in this coastal area must be caused by large-scale subsidence, possibly involved with the 500 mb ridge axis (Fig. 8), which is slightly to the west of the warming regions. The subsidence on the eastern side of



**Figure 30.** 850 mb horizontal thermal advection ( $1^{\circ}\text{K}/\text{day}$  contour interval) for 12UTC 9 June 1994 with positive (negative) values indicated with solid (dashed) lines.

the ridge could be responsible for this warming.

The initiation period of the CTD (12UTC 9 June to 12UTC 10 June) has predominant warming over the entire domain, except for a region south of the CB region. Areas of strong warming exist off northern CA and extend to the south and along the central CA coast (Fig. 26). The corresponding advection chart at 00UTC 10 June (Fig. 31) has a broad region of positive thermal advection extending off the central CA coast between SFO and Pt. Conception. However, strong cold advection is prevalent in northern CA and the western states. Because the warming temperature trend in northern CA corresponds well with the area of cold advection, subsidence must be contributing to the temperature rises. At this time, the 850 mb winds are light and northwesterly (Fig. 12), and the 700 mb winds (not shown) have a consistent on-shore component (westerly to southwesterly). As in the previous period, neither horizontal advection nor lee troughing can be responsible for the temperature rises over northern CA, and synoptic-scale factors must be operating to produce the subsidence in the area.

In the region south of the Channel Islands, a tongue of decreasing temperatures is ridging northward ( Fig. 26). A region of cold advection (Fig. 31) is evident across the region, which corresponds quite well to the temperature change and to the buildup and surge of stratus across the region at this time. Southerly 850 mb and 700 mb winds across this region appear to be aiding in the propagation of lower temperatures and stratus to the north.

The final period (00UTC 10 June to 00UTC 11 June) has strong warming off northern CA and slight cooling extending from the south along the central CA coast (Fig.

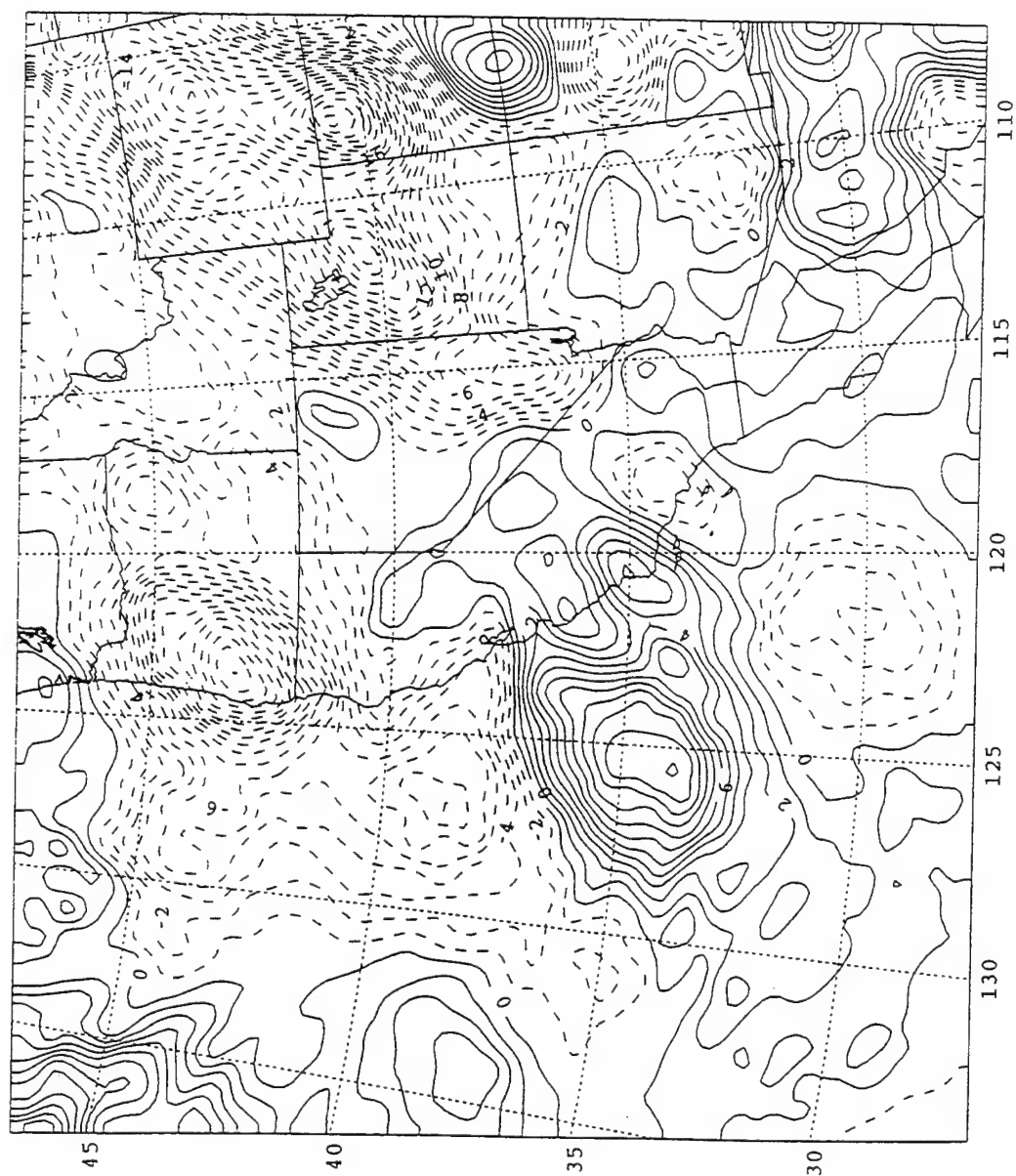


**Figure 31.** 850 mb horizontal thermal advection as in Fig. 30, except for 00UTC 10 June 1994.

27). The 850 mb thermal advection chart at 12UTC 10 June (Fig. 32) has a lobe of positive thermal advection extending off-shore from central CA and a maximum positioned near  $35^{\circ}N, 126^{\circ}W$  in that lobe. This corresponds well to the region south of MRY in which the trough moved off-shore and to the region where the low eventually developed at 00UTC 11 June (Fig. 16). Cold advection extends across the eastern Pacific and northern CA and additionally a negative area extends from the south over the Channel Islands. Thermal advection again does not correlate particularly well with the temperature changes in this plot. For example, the temperatures are rising off northern CA and extensive cold advection covers the region. The region of warm advection extending off the central CA coast does exist in the same areas that the low-level temperatures increase, but the temperature increase is not necessarily coincident with the advection. The 850 mb (Fig. 18) and 700 mb winds (not shown) have consistent on-shore flow that is not consistent with lee troughing in northern or central CA. This result indicates that synoptic-scale vertical motion is becoming more significant during the later phases of the CTD.



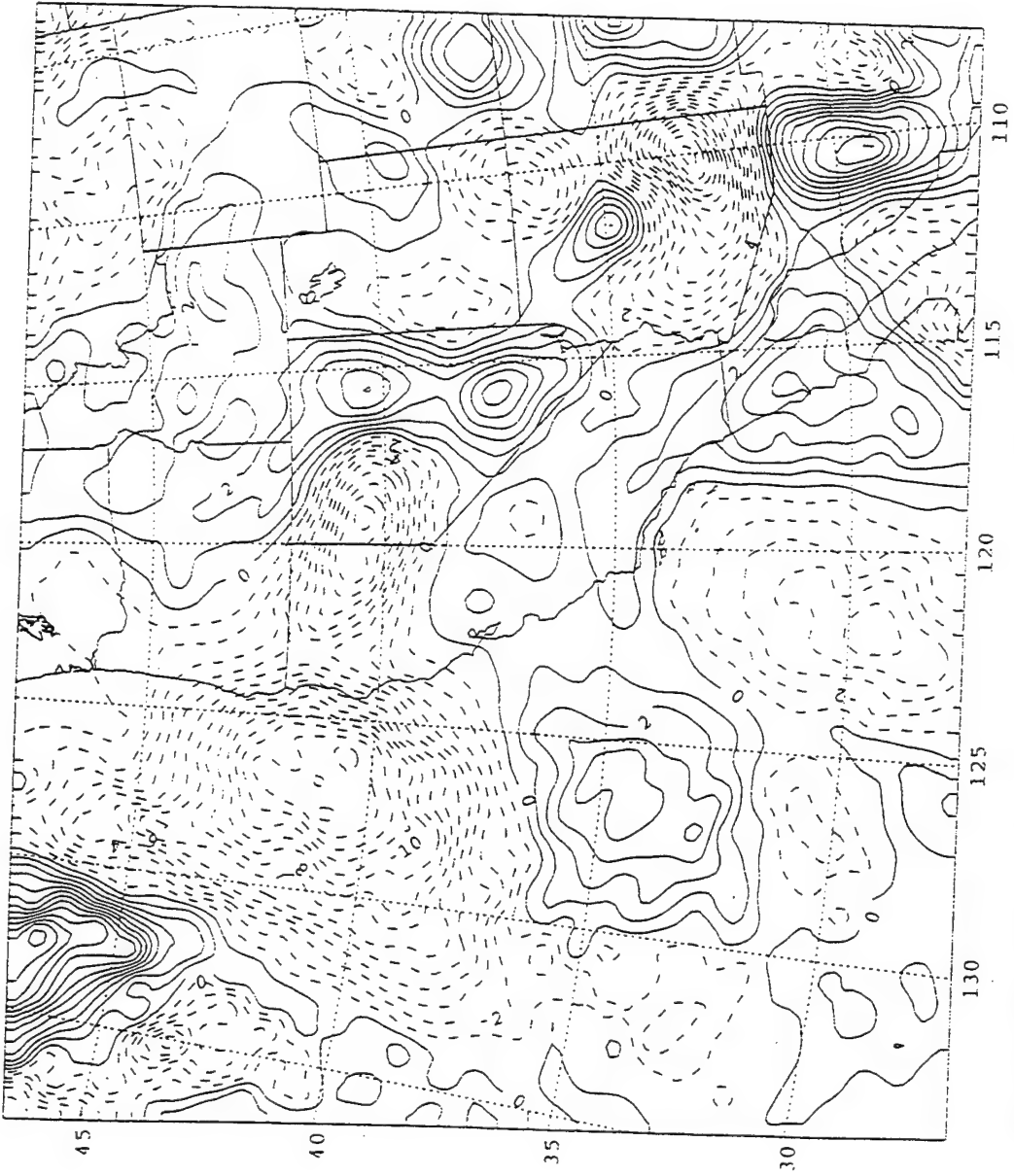


**Figure 32.** 850 mb horizontal thermal advection as in Fig. 30, except for 12UTC 10 June 1994.



## V. DISCUSSION

From the analysis of the SLP evolution and the diagnosis of the low-level temperature changes, several important refinements in our understanding of synoptic and MBL processes in a CTD event can be suggested. The most important refinement concerns the nature of the synoptic-scale processes that initiate the disturbance. The low-level heating results also have implications about the role of MBL depth and its evolution over time.

### A. INITIATION MECHANISM

Mass and Bond (1995) suggest that lee troughing causes the inland trough to shift towards the northern CA coast, which produces the south to north pressure gradient. The analyses of the 10 June 1994 CTD suggest that lee troughing may be responsible for shifting the trough to the coast in a relatively uniform manner. Thus, the trough axis continues to lie parallel to the coast, not across it as suggested by Mass and Bond.

Winds at 850 mb support lee troughing along the coastal mountains being a key in the migration of the thermal trough to its along-shore orientation and in the subsequent relaxation of the pressure gradient along the coast (Fig. 1). The 850 mb winds have a strong off-shore component during the pre-initiation phase (12UTC 9 June and 00UTC 10 June) as seen in Figs. 2 and 7. The orientation of the 850 mb winds across the central valley region of CA and proceeding across the coastal mountains would certainly induce lee troughing to the west of the coastal mountains. The lee troughing effects are greatly reduced by 00UTC 10 June, when the 850 mb winds decreased to less than 2 kt between SFO and Pt.

Conception. In addition, the coastal pressures generally rise along the coast after this time, with the exception of one area south of Monterey.

It is quite apparent from Fig. 9 that the first time the along-shore SLP gradient reversed was between Monterey and Pt. Conception at 06UTC 10 June, and was associated with the previously mentioned localized pressure minimum. As indicated above, reduction of the 850 mb off-shore winds (Figs. 7 and 12) 6 h preceding and following the SLP gradient reversal indicates that lee troughing is not responsible. Although winds at 850 mb may have a slight off-shore component, the magnitudes are vastly reduced ( $<2$  kt). The 850 mb thermal advection (Figs. 31 and 32) have strong, persistent regions of positive thermal advection south of Monterey. In this case, strong evidence exists that thermal advection at and below 850 mb is the key to the along-shore SLP gradient reversal and the initiation of the CTD.

Once the south to north along-shore pressure gradient south of Monterey was established, the winds responded by turning from northwesterly to southwesterly within a few hours. The strength of the predominant coastal inversion and the height of the coastal topography above the inversion acted to trap the southwesterly winds and force air to flow north along the coast in an ageostrophic down-gradient nature. At the initiation time and the 6 h thereafter, the winds near the coast appeared to be highly ageostrophic, and similar to the response suggested by Mass and Bond (1995) for synoptic-scale forcing.

Thermal advection at 850 mb, which was a key in the initiation of the CTD, was also important in changing the SLP gradient along the coast, and thus altering the forcing of the

CTD. The SLP analysis at 00UTC 11 June (Fig. 16) shows, for the first time, the development of a closed low near  $34^{\circ}$  N,  $143^{\circ}$  W. Development of this off-shore low pressure center changed the SLP gradient in the region from a south to north along-shore orientation to a gradient extending east to west (off-shore). That is, higher pressures existed over CA and lower pressures were off-shore. Therefore, the along-coast winds from the south were in the same direction as the geostrophic winds. Winds now appear more parallel to the isobars, which is suggestive to quasi-geostrophic flow relative to the cross-coast SLP pressure gradient. A Kelvin wave response would also have winds in quasi-geostrophic balance relative to the cross-coast SLP gradient. Although the MBL was not fully analyzed to determine its cross-coast evolution, the SLP changes suggest a MBL slope consistent with the Kelvin wave theory (sloping upward vertically towards the coast). During the progression of the CTD from 12UTC 10 June to 00UTC 11 June, a coastally trapped ageostrophic response to the along-shore SLP gradient changed to a more nearly geostrophic response to the large-scale, cross-shore SLP gradient.

## **B. MARINE BOUNDARY LAYER INFLUENCE**

Considerable debate has centered on the role of MBL height gradients versus synoptic-scale processes in establishing and maintaining the south to north pressure gradient. One of the keys to the Kelvin wave hypothesis is that the along-shore pressure gradient reversal is driven by the pressure rise associated with lifting of the MBL coincident with the surge. This analysis of the 10 June CTD suggests this is not the case at initiation, because the lowest SLP at 06UTC 10 June along the central coast south of Monterey is associated

with the strongest off-shore advection of warm air at 850 mb. Once this low pressure area is established, the southwesterly flow toward the coast most likely acts to lift the MBL inversion.

During the free propagation phase of the CTD, the difference in surface pressures along the coast between the CB region and SFO reached magnitudes between 2 mb and 3 mb. The surface pressure due to the increase in depth of the MBL will be calculated using the hypsometric equation

$$P = P_o \exp [g H / (R_d T_v)] \quad (6)$$

In this form,  $P$  and  $P_o$  are the pressures at the bottom and top of the layer respectively,  $H$  is the thickness of the layer, and  $R_d$  is the gas constant for dry air. The height of the MBL early on 10 June at the Ft. Ord profiler station (north of Monterey) was about 50 m (Fig. 33). As the CTD passed, the MBL lifted to near 350 m, so a nominal value of 300 m was used for the layer depth. Assuming a constant thickness of 300 m with  $T_v = 25^\circ \text{C}$  being replaced by a layer with  $T_v = 13^\circ \text{C}$  the surface pressure would increase by 1.6 mb, which accounts for  $\sim 50\%$  of the along-shore pressure gradient changes observed. During passage of the CTD, a buoy south of Monterey observed pressure rises of 3.5 mb. Although the deepening of the MBL has a large role in the pressure rises as the CTD progresses along the coast, the MBL deepening cannot fully account for the magnitude of the along-shore pressure changes associated with the SLP gradient reversal.

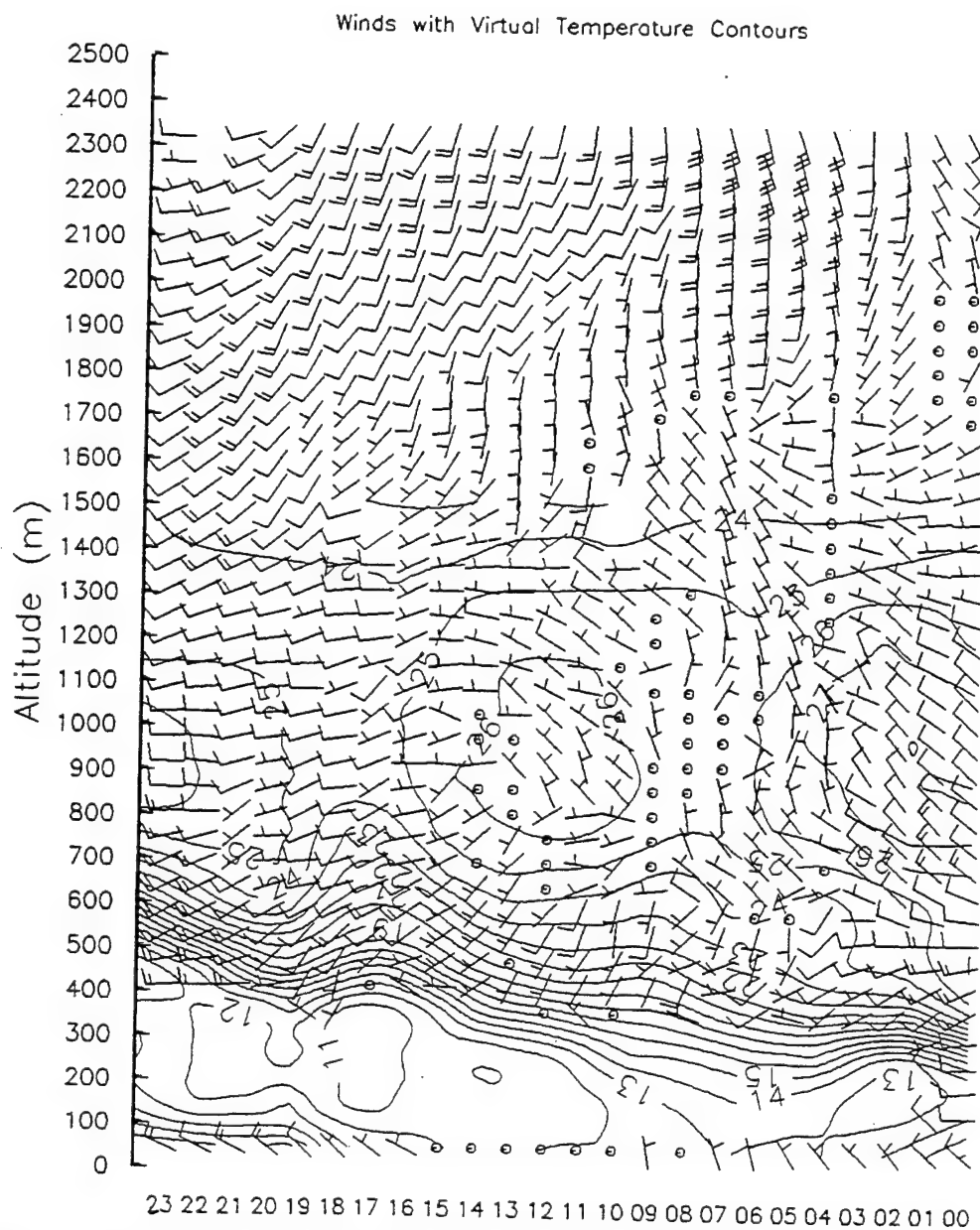


**Figure 33.** 915 MHz radar wind profiler observations (full barb 10 kt, half barb 5 kt) and virtual temperature (solid lines  $1^{\circ}\text{C}$  contours) at Monterey, CA from 00UTC 11 June (right axis) to 23UTC 11 June (left axis). Winds  $< 2$  kt not shown.





## VI. CONCLUSION AND REMARKS

This study described several important factors in coastally trapped disturbances. An in-depth and accurate SLP evolution of the CTD life cycle was completed. Lee troughing was found to be a factor in the movement of the central CA thermal trough to parallel the coastal region, which relaxed the along-shore SLP gradient, but did not initiate the CTD event. Key to the initiation of the CTD was the movement of the thermal trough off-shore and reversal of the along-shore SLP gradient south of Monterey, which appears to be tied to low-level warm advection in that region. The continued thermal advection off the central CA coast aided in the development of an off-shore low center that altered the propagation mechanism in the surge from ageostrophic down-gradient flow to a geostrophic response as the along-shore SLP gradient relaxed.

The present study was hampered by a lack of complete 4-dimensional analyses and a sparse observation set over the ocean. In view of the assumptions required in this study, several areas need to be investigated to obtain a more complete understanding of this complex event. Detailed studies of the vertical motion fields in upper levels for this and other CTD cases must be completed using complete 4-dimensional analyses or models to establish the relative importance of horizontal thermal advection and subsidence warming throughout the event. In addition, similar techniques should be focused on the MBL to better understand the complex dynamics in the MBL that evolve and may enhance or force the CTD's initiation and propagation. These studies require more complete sets of

observations off the coast.

Although this study was not specifically a forecasting thesis, it is apparent that since synoptic scale forcing is an important feature in the initiation of this particular CTD, current operational models should perform reasonably well in forecasting the event. Future studies need to include the adjudication of various operational models in their ability to correctly forecast a CTD. The ability to correctly forecast a CTD is paramount for any forecaster operating in this complex environment, as it would directly affect the safety of a ship and her crew.

## LIST OF REFERENCES

- Bond, N. A., C.F. Mass, and J. E. Overland, 1995: Coastally trapped southerly transitions along the U.S. west coast during the warm season. Part I: Climatology and temporal evolution. *Mon. Wea. Rev.* (in press).
- Carcena, F., 1987: Analytic approximation of discrete field samples with weighted sums and gridless computation of field derivatives. *J. Atmos. Sci.*, **44**, 3753-3768.
- Dorman, C. E., 1985: Evidence of Kelvin waves in California's marine layer and related eddy generation. *Mon. Wea. Rev.*, **113**, 827-839.
- Dorman, C. E., 1987: Possible role of gravity currents in Northern California's coastal summer wind reversals. *J. Geophys. Res.*, **92**, 1467-1488.
- Durkee, P. A., 1994: Monterey Area Shiptrack Experiment [CNO Project K-1420] Science plan. *Naval Postgraduate School*, 44 pp.
- Madych, W. R., and S. A. Nelson, 1990: Multivariate interpolation: A variation theory. *J. Approx. Theory Appl.* **4**, 77-89.
- Mass, C. F., and M. D. Albright, 1987: Coastal southerlies and alongshore surges of the west coast of North America: Evidence of mesoscale topographically trapped response to synoptic forcing. *Mon. Wea. Rev.*, **115**, 1707-1738.
- Mass, C. F., and M. D. Albright, 1988: Reply. *Mon. Wea. Rev.*, **116**, 2407-2410.
- Mass, C. F., and N.A. Bond, 1995: Coastally trapped southerly transitions along the U. S. West coast during the warm season. Part II: Synoptic evolution. *Mon. Wea. Rev.* (in press).
- Nuss, W. A., and D.W. Titley, 1993: Use of multiquadric interpolation for meteorological objective analysis. *Mon Wea. Rev.*, **122**, 1611-1631.
- Reason, C. J. C., and D. G. Steyn, 1992: The dynamics of coastally trapped mesoscale ridges in the lower atmosphere. *J. Atmos. Sci.*, **49**, 1677-1692.



## INITIAL DISTRIBUTION LIST

|    |  | No. Copies |
|----|--|------------|
| 1. | Defense Technical Information Center<br>Cameron Station<br>Alexandria, Virginia 22304-6145   | 2          |
| 2. | Library, Code 52<br>Naval Postgraduate School<br>Monterey, California 93943-5101   | 2          |
| 3. | Superintendent<br>Attn: Chairman, Department of Meteorology (Code MR/HY)<br>Naval Postgraduate School<br>Monterey, California 93943-5000 | 1          |
| 4. | Superintendent<br>Attn: Chairman, Department of Oceanography (Code OC)<br>Naval Postgraduate School<br>Monterey, California 93943-5000   | 1          |
| 5. | Superintendent<br>Attn: Professor Wendell A. Nuss (Code MR/Nu)<br>Naval Postgraduate School<br>Monterey, California 93943-5000           | 1          |
| 6. | Superintendent<br>Attn: Professor Russell Elsberry (Code MR/EL)<br>Naval Postgraduate School<br>Monterey, California 93943-5000          | 1          |
| 7. | Lieutenant Paul S. Oosterling<br>765 Ridge Rd.<br>Ontario, New York 14519  | 2          |
| 8. | Superintendent<br>Naval Research Laboratory<br>7 Grace Hopper Avenue Stop 2<br>Monterey, California 93943-5502                           | 1          |

- |     |   |   |
|-----|---|---|
| 9.  | Chairman<br>Oceanography Department<br>U. S. Naval Academy<br>Annapolis, Maryland 21402   | 1 |
| 10. | Office of Naval Research (Code 420)<br>800 N. Quincy Street<br>Arlington, Virginia 22217  | 1 |
| 11. | Library<br>Scripps Institution of Oceanography<br>P. O. Box 2367<br>La Jolla, California 92037  | 1 |
| 12. | Chief, Technical Procedures Branch<br>National Weather Service<br>National Oceanic and Atmospheric Administration<br>Silver Springs, Maryland 20910 | 1 |
| 13. | NOAA Library<br>7600 Sand Point Way NE<br>Building 3<br>Seattle, Washington 98115   | 1 |